This is to certify that the

thesis entitled

EXPERIMENTAL AND NUMERICAL INVESTIGATIONS OF STAMP HYDROFORMING AND IRONING OF WRINKLING IN SHEET METAL FORMING

presented by

Nader Elias Abedrabbo

has been accepted towards fulfillment of the requirements for

M.S. degree in Mechanical Engineering

F. Pourboghrat

Major professor

Date 6/7/02

EXPERIMENTAL AND NUMERICAL INVESTIGATIONS OF STAMP HYDROFORMING AND IRONING OF WRINKLING IN SHEET METAL FORMING

By

Nader Elias Abedrabbo

A THESIS

Submitted to
Michigan State University
in partial fulfillment of the requirements
for the degree of

MASTER OF SCIENCE

Department of Mechanical Engineering

2002

ABSTRACT

EXPERIMENTAL AND NUMERICAL INVESTIGATIONS OF STAMP HYDROFORMING AND IRONING OF WRINKLING IN SHEET METAL FORMING

By

Nader Elias Abedrabbo

The goal of this study was to verify, experimentally and numerically, that the stamp hydroforming process is a suitable alternative to conventional stamping as a means for producing defect-free sheet metal parts. The pressurized fluid used in stamp hydroforming is shown to have the effect of increasing the forming limits of materials; that is deeper drawing depths are achieved without rupture. Also, using a specific pressure profile, wrinkle-free parts with deeper draws could be produced. Stamp hydroforming involves supporting the sheet metal with a bed of pressurized viscous fluid during the entire forming process. The external support provides a through-thickness compressive stress that delays the onset of tearing and wrinkling. Stamp hydroforming experiments with a hemispherical punch were conducted using the Interlaken double-action stamping press. Numerical analysis was conducted using the explicit finite element code LS-Dyna 3D. The accuracy of the numerical model was first established and fine-tuned using experimental data. The numerical model was then used to explore new forming ideas not currently possible with the present experimental setup. A new blank holder design is suggested from these numerical results.

To My Family

ACKNOWLEDGMENTS

I would like to thank my advisor Dr. Farhang Pourboghrat, my colleagues, especially Michele Zampaloni, for the assistance that they have provided during the course of my study in pursuit of my Masters of Science degree. Also, to the J. William Fulbright Foreign Scholarship Board for their grant that enabled me to pursue my studies at MSU as a Fulbright Scholar. Also, for AMIDEAST for their efforts and continued dedication in supporting the Fulbright grantees during their studies.

TABLE OF CONTENTS

LIST OF TABLES

LIST OF FIGURES

LIST OF ABBREVIATIONS

σ - Cauchy Stress

k - Strength Coefficient

ε - Cauchy strain

n - Work Hardening Exponent

σ_y = Yield Stress

Φ - Yield Function

S_1, S_2 & S_3 are the Principal Values of the Stress Deviator

s – Fourth Order Tensor

L – Fourth Order Linear Operator

c_1, c_2, c_3, α_1, α_2, α_3 - are Material Coefficients

P - Transformation Matrix

Chapter 1

INTRODUCTION

Sheet metal stamping uses a male (punch), a female and a blank holding die, to plastically (permanently) deform a blank sheet of metal into a desired shape. This technique is widely used in order to fabricate thousands of sheet metal structures per day in several industries, e.g. automotive, aerospace, beverage industry etc.... Depending upon several factors such as geometry, volume and material type, deep drawing or stretch forming is used as different methods to form sheet metals [1]. In sheet-forming processes however, several types of failures could occur, such as rupturing, necking, wrinkling and springback [2], that are undesirable. Also, there are significant expenses associated with the necessary tooling and the success of the process largely depends on the ingenuity of skilled machinists to bring the economic costs down to suitable levels.

Sheet metal stamp hydroforming is currently being considered as a viable alternative to conventional sheet metal stamping. Stamp hydroforming offers many advantages over conventional stamping when fabricating difficult-to-form parts. The advantages of stamp hydroforming are numerous and the process is receiving significant attention from both automotive and aerospace industries. These advantages include improved formability due to the applied fluid pressure, low wear rate of tools, better distribution of plastic deformation, significant economic savings due to using less number of tooling, and finally the potential for reduced amount of finishing work required [7].

In stamp hydroforming, one or both surfaces of the sheet metal are supported with a pressurized viscous fluid to assist with the stamping of the part and a female die is not required. The pressurized fluid serves several purposes:

(1) Supports the sheet from the start to the end of the forming process, thus yielding a better formed part,

(2) Delays the onset of material failure, and

(3) Could potentially reduce wrinkle formation when applied to one or both sides of the sheet metal.

McClintock (1968) [3], Rice et al. (1969) [4], Clift et al. (1990) [5] and Hartley et al. (1992) [6] demonstrated that for sheet metals, the use of a hydrostatic pressure prevented the initiation and spreading of microcracks within the metallic material. Based on the success found using a hydrostatic pressure to delay the onset of fracture, the idea of stamp hydroforming was investigated as an alternative method for conventional stamping. The hydroforming process is used to form sheet metals that would be difficult to form using the traditional forming processes where instabilities and failures may occur.

The sheet metal stamp hydroforming method, shown in Figure 1, is a process in which a part is formed by a simple hemispherical punch. The workpiece is placed on the clamping mechanism, as shown in Figure 1.1. Figure 1.2 shows the upper fluid chamber being lowered and the workpiece clamped securely between the two die halves, creating a seal for the upper fluid chamber. The fluid is then injected into the upper chamber and given an initial pressure.

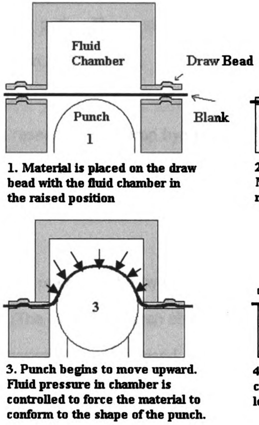

Figure 1. Schematics of a hydroforming press using a hemispherical punch with a blank holding support.

As the punch moves up, the sheet metal begins to deform and take on the shape of the punch, in this case a hemispherical shape, as shown in Figure 1.3. The pressure in the upper chamber is controlled via a pressure transducer and is used as a means of forcing the sheet to conform to the shape of the punch. Once the punch reaches the prescribed depth, the fluid is drained and the chamber is raised, as shown in Figure 1.4, to remove the formed part from the die.

The challenge in using sheet hydroforming process lies in finding an appropriate fluid pressure-punch stroke path, which will avoid rupturing or wrinkling the sheet metal. There have been numerous studies done to identify this optimum path. These studies will be discussed in detail in the literature review section, in Chapter 2.

In this research, the stamp hydroforming process is investigated as a means for shaping aluminum alloy sheet metals with the objective of achieving higher draw-depths and forming wrinkle-free parts using fluid pressure.

Literature review of the hydroforming process and wrinkling is presented in chapter 2. The overall research objectives are presented in chapter 3. In chapter 4 the experimental setup used in the research and an explanation of the experiments performed with some results are presented. Setup of the numerical analysis performed with explanation of some important issues encountered during the research is presented in chapter 5. The majority of the results and the comparison between the experimental and numerical analysis are presented in chapter 6. Some conclusions are made in chapter 7.

Chapter 2

LITERATURE REVIEW

Numerous studies have been conducted on traditional sheet metal stamping methods such as mechanical stretch forming and deep drawing where both methods requiring a male and a female die for the proper forming of a finished part. Much less literature is available on the sheet metal stamp hydroforming process, which uses a punch and hydrostatic fluid pressure to form a finished part. In this chapter a review of the literature focusing on the most recent experimental and numerical studies conducted on sheet metal stamping and sheet hydroforming processes will be presented.

2.1 Sheet Metal Hydroforming Literature Review

McClintock (1968) [3] and Rice et al. (1969) [4] conducted studies on sheet metals demonstrating a rapid decrease in fracture ductility as a hydrostatic pressure, applied across the material, was increased. Clift et al. (1990) [5] and Hartley et al. (1992) [6] demonstrated that for sheet metals, the use of a hydrostatic pressure prevented the initiation and spreading of microcracks within the metallic material.

Yossifon and Tirosh (1977–1988) [8–12] published a series of articles dealing with simple analysis of the hydroforming deep drawing process as applied to the formation of cups from metallic materials such as copper, aluminum, steel and stainless steel. The goal of the studies was to establish a hydroforming fluid pressure path, relative to the punch stroke, that would prevent part failure due to rupture or to wrinkling. Their earlier studies demonstrated the effect that excessive and insufficient fluid pressures have on the premature failure of hydroformed parts. The purpose of the later investigations was to determine a predetermined path that can be followed to produce parts that are free from these types of defects.

In order to minimize wrinkling instabilities the fluid pressure was held to the possible minimum. The pressure relationship, based on equating the bending energy of the buckled plate and the work against lateral load (spring-type blankholder or fluid pressure) to the work done by the in-plane compressive membrane forces, included the governing parameters of friction coefficient and anisotropy. Through their work they were able to show that rupture instabilities occur when the fluid pressure being used for the hydroforming process was too high. The fluid pressure constrained the motion of the part and forced the punch through the material. The fluid pressure to prevent rupture was evaluated in terms of average friction coefficient, material properties, and geometrical considerations. Using these two fluid pressure values a range was determined that allowed for the manufacture of parts without the occurrence of wrinkling or rupturing. This theory was tested experimentally and the results were very favorable with the predicted outcomes.

Lo, Hsu and Wilson (1993) [13] expanded upon the earlier work of Yossifon and Tirosh by applying the deep drawing hydroforming theory to the analysis of the hemispherical punch hydroforming process. The purpose of this work was to determine a theoretical method of predicting failure due to wrinkling (buckling) or rupture (tensile instability) during the punch hydroforming of hemispherical cups. This work was basically an extension of the work done by Yossifon and Tirosh by incorporating a general friction-force expression into the analysis and expanding to more complicated geometries.

In order to predict failure the part was split into three regions based on the geometric characteristics of this operation. First there was a region where the part was free from contact with the die, a second region that consisted of the unsupported area termed the "lip area", and the third region that was the area of the part that had already come into contact with the surface of the punch. Along with the determination of the failure areas, the study also attempted to identify an upper and lower bound for manufacturing, a region termed the "work zone". It was proposed that if processes were run within these limits then there should be limited potential for failure. They were able to conclude that the working zone could be expanded by low friction forces, high strain hardening exponents, small drawing ratios, thick workpieces, and through the use of orthotropic materials.

Hsu and Hsieh (1996) [14] attempted to verify the theory developed by Lo, Hsu and Wilson through a series of experimental procedures. The purpose was the validation and verification of the failure prediction method for wrinkling and rupture instabilities during the punch hydroforming of sheet metal hemispherical cups. Various hydroforming pressure paths were tested during the process to validate the theory. They determined conclusively that a path that intersected the lower boundary of the working zone would lead to premature material failure due to wrinkling in every case. The same result was found for the pressure paths that intersected the upper boundary of the working zone. Through a series of varying parameter experiments the results achieved experimentally were very comparable to the theoretical predicted results.

Gelin, Delassus and Fontaine (1994) [15] experimentally and numerically studied the effects of process parameters during the aquadraw deep drawing process. The purpose of the study was to determine the main parameters that influence the aquadraw deep drawing process, specifically, the determination of the pressure in the cavity and under the blankholder as functions of process geometry, material parameters, and fluid parameters. Aquadraw deep drawing differs from hydroforming due to the use of a thin layer of water, subjected to fluid flow that replaces the thin rubber diaphragm between the material and the die cavity. The investigation, limited to axisymmetric sheet metal materials, proposed a cavity pressure modeling technique based on the optimal parameters of the process instead of being modeled by the Reynolds equation.

A relationship to determine the cavity pressure was also derived based on the material behavior, the material thickness, the die entrance radius, and the drawing ratio. The paper evaluated the influence of each of these parameters on the overall cavity pressure. To demonstrate the effectiveness of these parameters on the determination of the cavity pressure, the study referenced other researcher's experiments. Numerical analysis predictions of the deep drawing process were in good agreement with the experimental behavior of the parts analyzed.

Gelin, Ghouati and Paquier (1998) [16] and Baida, Gelin and Ghouati (1999) [17] both expanded upon the numerical work conducted in the Gelin, Delassus and Fontaine work dealing with the aquadraw deep drawing process. These two investigations expanded upon the numerical work by adding the process parameters monitoring, identification tools and general sensitivity analyses to the numerical method used as a predictor of the die cavity pressure during the deep drawing process. Overall their respective results showed very good correlation between the numerical and experimental behavior of the material.

Shang, Qin and Tay (1997) [18] spent time on the evaluation of the copper spherical shell hydroforming process by studying the effects of intermittent draw-in during the operation. The purpose of this investigation was to examine, experimentally and numerically, the effects these intermittent changes would have on the formability of the blank material. During the processing of the cups there were two main formability factors that were investigated; the radius of the die shoulder and the blank holding force. Reducing the die shoulder radius increased formability but the use of a small radius had the potential of causing premature tearing of the blank along the die shoulder. Reducing the blank holding load encouraged draw-in, inward flow of the flange material, thereby increasing the average thickness of the product and delayed the onset of material failure.

Since the radius of the die shoulder is normally fixed or limited by the product specifications then the logical approach to increasing formability would be to vary the blank holding load. During this study the copper material was formed into a nearly spherical shell using four different approaches. The first approach was a single-stage hydroforming process using two different deformation paths, one that allowed for the draw-in of the flange, and one that did not allow the draw-in to occur. The second approach evaluated the effect of a double-stage hydroforming process also using two different flow paths. The first path allowed for the draw-in during the first stage, and restricted it in the second. The second path was just the opposite, draw-in was not allowed during the first stage yet was permitted during the second stage. The results showed that during the single-stage hydroforming process, the formability of the material was greatly improved. For the double-stage hydroforming operation, the best results were achieved during the path that did not allow for the draw-in of the flange during the first stage, but did during the second stage.

2.2 Wrinkling Literature Review

Wrinkling in sheet metal forming, with tearing, is one of the most important instabilities that occur in parts formed using stamp forming and deep drawing processes. This phenomenon limits the type of parts and geometries that can be formed using these techniques. Simulation of wrinkling behavior using the finite element method (FEM) in sheet metal stamping is an important predictive tool. An accurate finite element model that could accurately predict the formation of wrinkling could also be used at the tooling design stage of parts of various shapes.

Many studies have been made to study the wrinkling behavior in sheet metal forming. These could be traced back to Geckler [20], Baldwin et al. [21], Senior [22], Yoshida [23] and others. Triantafyllidis and Needlmen (1980) [24] studied the effect of compressive bifurcation instabilities on the onset of flange wrinkling using the Swift cup test. Using numerical analysis linked with previous experimental work, they established the limiting drawing ratios (LDR), defined as the largest drawing ratio from which a cup can be drawn without fracture. The critical conditions governing the onset of wrinkling were studied.

Many researchers have studied simulation of wrinkling behavior in sheet metals using the FEM (Finite Element Method) method. Doege et al. (1995) [25] studied the necking and wrinkling behavior using several techniques. Necking, caused by tensile instability, was studied utilizing the results of the Continuum

Damage Mechanics (CDM) and using the Gurson constitutive model. For studying the wrinkling behavior, they start by studying the buckling of one-dimensional long column. The FEA method was used, where the problem was solved both implicitly and explicitly. Numerical results were then compared against experimental results of deep drawing of a 50mm cup. Necking behavior requires taking into account of the material microstructure, in particular microscopic processes that precede rupture. Therefore, the Gurson model, which accounts for the microscopic processes, was used.

Wrinkles that form during the sheet forming are due to internal compressive instabilities. Two types of wrinkles occur (i) wrinkles of first order in the flange; and (ii) wrinkles of second order in the free-forming (unsupported) zone between the punch radius and the die radius. Since wrinkling is a problem of equilibrium state, the prediction of wrinkles is more difficult for implicit codes than for explicit codes. Introducing statistical geometrical imperfections in the blank is necessary in order to be able to simulate the wrinkling behavior using the implicit method.

Boyce and Cao (1997) [1], and Wang and Cao (2000) [26] studied the problem of wrinkling simulation using the implicit and explicit methods. Using the ABAQUS-implicit code the problem of forming a square cup was studied. Also Ls-Dyna explicit code was used. In order to solve the problem using the implicit code, initial imperfections had to be introduced into the blank mesh to take into account the instabilities. No imperfections were introduced in the explicit part of the analysis.

Using these results they showed that the implicit FEM model with shell elements may overwhelmingly overpredict the failure heights, and the predictions of the explicit FEM models are sensitive to the selected critical wrinkling heights, the mesh density, the punch velocity, etc.

Chung and Shah (1992) [27] numerically studied sheet metal forming of anisotropic materials. Since wrinkling is a geometrical and a material dependent phenomenon, an anisotropic constitutive model was used. The anisotropic constitutive model introduced by Barlat et al. [28] was used in this study. Prior to this work, finite element analyses assumed material isotropy in their simulations, although the sheet metals usually showed anisotropic properties. Using experimental and numerical studies using ABAQUS of the cup drawing test using AA2008-T4 material, they show the importance of using the correct constitutive model in representing material behavior in sheet metal forming processes using the explicit method. And the accuracy that could be achieved using this model versus experimental data was established.

Several other studies have been also made, such as Kim et al. [29-30], Kawaka et al. [31]. In these papers, verifying numerical data against experimental ones the importance of using the correct constitutive model in the FEM analysis to represent anisotropic behavior of the material was shown.

Chapter 3

RESEARCH OBJECTIVES

The objectives of this research were to study, experimentally and numerically, the effects of applying fluid pressure would have on improving the formability of aluminum sheet metals and reducing the failure modes that appear in conventional sheet stamping. More specifically, the following improvements associated with the sheet hydroforming process were investigated:

1. Increasing draw depths before rupturing of aluminum sheet metals,
2. Eliminating the wrinkling failure, especially in the deep drawing of aluminum sheets, and
3. Calculating an optimum fluid pressure-punch stroke profile to form aluminum sheet metals without any defects.

Challenges that are present during the stamp hydroforming process can be classified into three broad categories: material, geometrical and fluid pressure. The material challenge refers to the choice and behavior of the sheet metal. One of the major obstacles concerns the delicate balance between the fluid pressure and the ductility of the material chosen for the hydroforming process. The fluid pressure needs to be high enough to stretch and bend the work piece through its radius of curvature to conform to the shape of the punch yet the material needs to be ductile enough to form without rupturing.

The second challenge is the geometrical effects, this relates to the specific geometry of the part and the relationship with the forming tools. Also, it can include the method in which the part is formed, i.e., stamping or deep drawing. Geometrical effects and the deep drawing of the sheet metal into the die cavity, causes some portions of the sheet to be unsupported during the forming process. The formation of compressive hoop stresses in the unsupported portions of the sheet metal cause wrinkling followed by eventual tearing of the sheet metal. Preventing these failure modes from occurring are particularly critical to automotive and aerospace industries where wrinkle-free parts are expected to be formed the first time.

The third challenge is the relationship between the fluid pressure and the punch stroke during the process. As shown by Yossifon and Tirosh [7-12] fluid pressures within the upper fluid chamber that are too high will cause the material to bend to the radius of curvature of the punch much faster than the ductility of the material may allow. This will lead to premature rupturing of the sheet metal. On the other hand, if the fluid pressure is too low the sheet metal may not stretch enough during the process and wrinkle.

Therefore, there is the need to establish an upper and lower limit on the fluid pressure, as it relates to the punch stroke, to determine an optimum fluid pressure-punch stroke path to ensure limited rupturing and wrinkling failures of the finished part. In the stamp hydroforming of sheet metals the difficulty lies in finding this appropriate fluid pressure-punch stroke path while avoiding rupturing and wrinkling instabilities. Lo et al. (1993) [11] and Hsu et al. (1996) [12] performed a series of experiments and analyses that established this fluid pressure-punch stroke path for the stamp hydroforming of metallic hemispherical cups. A generalized curve is illustrated in Figure 2 to help demonstrate one of the goals of the numerical and experimental research; the determination of the optimum fluid pressure-punch stroke path for the stamp hydroforming of aluminum sheet metals.

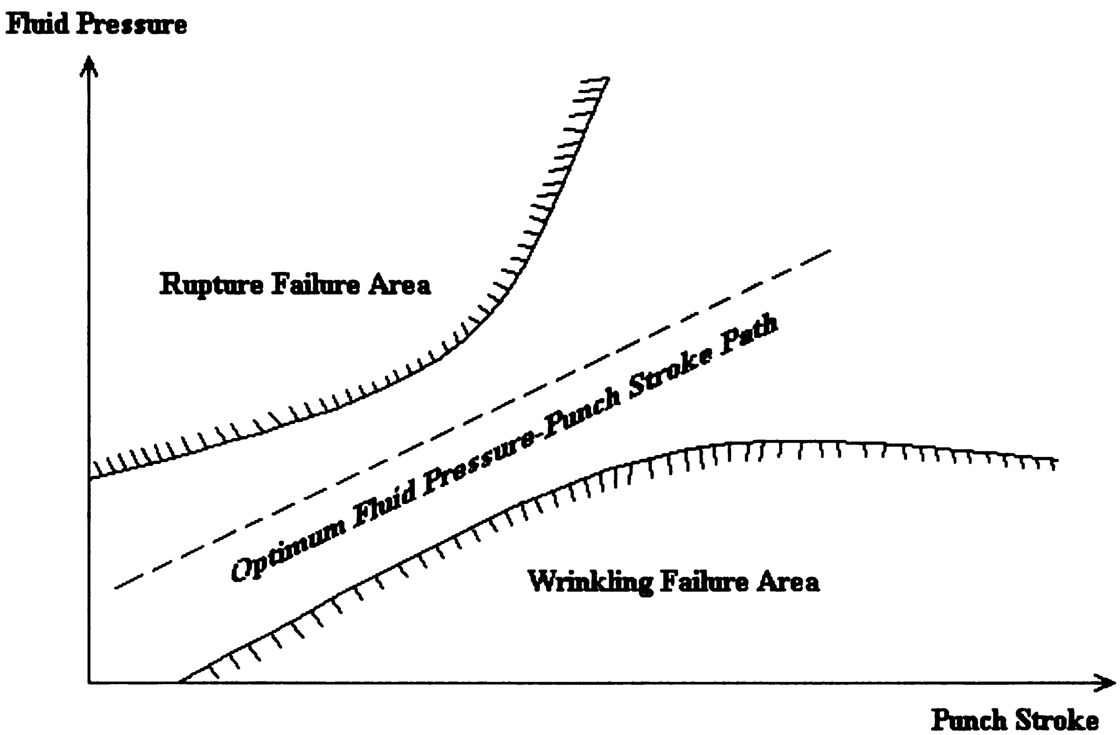

Figure 2. Generic curve illustrating the optimum fluid pressure-punch stroke path for the stamp hydroforming process.

Materials investigated in this research were 3003-H14 and 6111-T4-aluminum sheet alloys. These sheet materials were originally fabricated by ALCOA and supplied to us by GM and Ford through the Manufacturing Research Consortium (MRC) at MSU. Two hemispherical punches with 101.6mm (4in) and 76.2mm (3in) diameters were also used in this research.

Numerical analysis of the stamp hydroforming process was carried out using the explicit finite element code Ls-Dyna 3D. At first the simulation results were established qualitatively and then fine-tuned by comparing with the experimental data. The model was then used as a design tool to study new stamp hydroforming ideas where an experimental setup was not available. Finally, a new deep-drawing hydroforming blank holder was designed and built with the help of the results acquired through numerical modeling.

Chapter 4

EXPERIMENTAL WORK

In this section, the experimental apparatus for sheet hydroforming will be described, followed by a discussion of some of the experimental results obtained using the two hemispherical punches with 101.6mm (4in) and 76.2mm (3in) diameters.

4.1. Experimental Apparatus

The apparatus used in these experiments was built around an Interlaken 75 double action servo press, Figure 3, manufactured by Interlaken Technology Corporation, Eden Prairie, Minnesota. The double action refers to the clamping mechanism moving independently of the punch mechanism. This allows for the boundaries of the sheet blank to be clamped while the punch pushes the sheet into the die cavity filled with supporting fluid. The ability to independently control both the clamp and the punch affords the opportunity for various modifications of the experimental procedure.

The apparatus uses the LDH (Limiting Dome Height) setup used in industry for the evaluation of lubricants in the sheet metal. Some modifications were made to change the setup to research requirements. A thesis submitted by Zampaloni M. [32] has all the details about how the experimental setup was built.

The LDH die is essentially a pair of cylinders that are clamped together after placing a draw blank between them. The punch moves through one chamber, meets the material and stretches it into the second cylinder. The clamping mechanism typically contains a draw bead that would cause the sheet metal to get stretched only. Figure 4 shows a schematic drawing of the simple LDH die set that was used prior to modifications for the hydroforming process.

Figure 3. Double action servo press 75 manufactured by Interlaken Technology Corporation, Eden Prairie, MN.

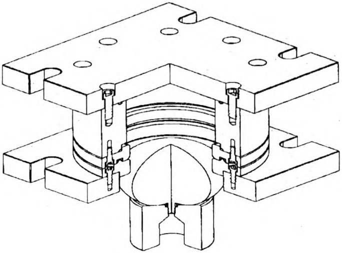

Figure 4. Schematic of a simple limiting dome height (LDH) test die set.

The experimental setup used for studying stamping, and one-sided pressure hydroforming, after the modifications, is shown in Figure 5. The die was retrofitted with four ports; one for measuring the pressure within the fluid cavity, one for injecting fluid into the die cavity, one for removing the air from the chamber during the fill process and one that is used to measure the fluid temperature within the chamber during the process. Figure 6 shows a schematic illustration of these changes while Figure 7 shows a picture of the in-house designed die that was used for studying the hydroforming process.

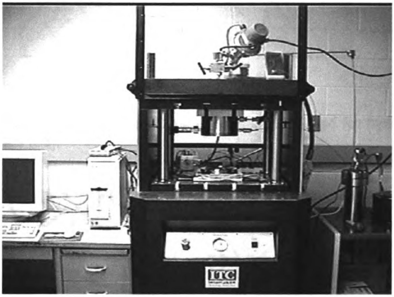

Figure 5. The modified Interlaken servo press 75 used for the hydroforming of aluminum sheets.

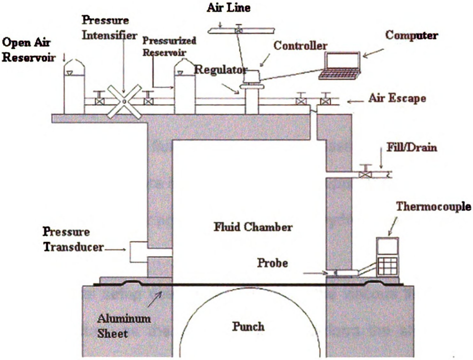

Figure 6. Schematic view of the experimental apparatus used for hydroforming hemispherical Cups [33].

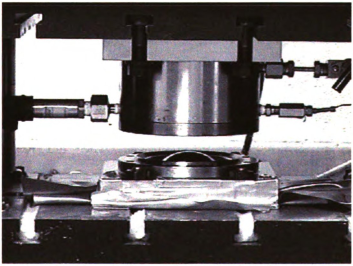

Figure 7. The in-house designed die set for hydroforming aluminum sheets.

Attached to the fluid line is a regulator/controller that is used to accurately control the fluid pressure within the die cavity, as the sheet metal is stamp hydroformed, as shown in Figure 8. If the fluid pressure is higher than a user-defined pressure profile, then the fluid is drained and the pressure in the system is reduced to the appropriate level. If the pressure is too low then the regulator pulls additional pressurized fluid from a pressure vessel that is in line with the rest of the system. A pressure intensifier is used to supply the necessary volume and pressure to the reservoir prior to the start of the hydroforming process.

The experimental setup used vegetable oil as the viscous fluid. Due to its incompressible nature, as the punch began to deform the sheet metal, the volume in the fluid chamber decreased causing the pressure to increase. A new petroleum based fluid, Novacool 9034, will be used for future experiments. The details of the user-defined pressure profile will be discussed in the numerical section.

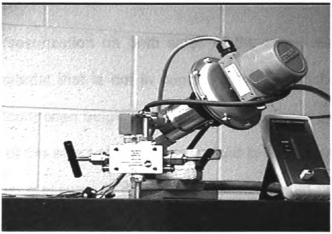

Figure 8. Regulator and controller used for the control of the fluid pressure within the forming chamber.

In an attempt to explore different design ideas, the process was conducted using a thin vinyl sheet in place of the counteracting fluid. By placing a vinyl material, which was stiff but also stretchable, over the sheet metal the effect of a localized hydrostatic pressure was simulated. As the punch moved into the sheet metal the vinyl counteracted the motion and added a pressure at the location of the sheet- punch contact area. Due to its stiffness, the unsupported regions of the sheet metal were unaffected by the use of this vinyl sheet, therefore, there were no bulging in the reverse direction.

A new experimental die, illustrated in Figure 9, was designed that would offer several advantages over the previous die design. The new die fills the sealed bottom chamber with fluid that is equalized with the fluid in the upper chamber. As the pressure in the upper fluid chamber increases due to the volume change, the displaced fluid will be forced into the bottom chamber thereby equalizing the pressure between the chambers (with a minute delay).

This equal pressurization on both sides of the sheet metal allows for the support of the material that is not in contact with the punch and prevents the sheet from an uncontrolled bulging in these regions. This new design will allow the investigation of the effect of applying the fluid pressure on both sides of the blank. Either equal pressure, or differential pressure could be applied between both sides of the blank. In the case of equal pressurization, the material that is in contact with the punch will experience a pressure that is representative of the localized hydrostatic pressure applied by the vinyl sheet, resulting in deeper draw depth prior to material failure. This new die design should also be able to use fluid pressures above the limiting 3848 kPa (558 psi) pressure with the current one-sided die design.

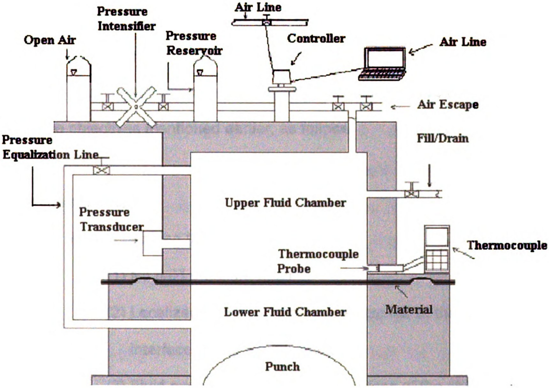

Figure 9. The new die design that would allow the pressurized fluid to be applied on both sides of the sheet metal [33].

4.2. Targeted Experiments

In order to learn about the effects that fluid pressure has on the formability of sheet metals during the stamp hydroforming process, both experimental and numerical studies were conducted. The experiments were carried out using four-inch and three-inch hemispherical punches. Two types of initial blank shapes were used, a 1 mm thick, square blank of 178mm x 178mm (7in x 7in), and a round blank of 178mm (7in) diameter. The blank materials used were 3003-H14 and 6111-T4 aluminum alloy sheets. Specific tests were carried out in order to establish the objectives mentioned earlier, as follows:

I. Experimental Studies:

   A. Pure Stretching (Stamp Forming):

      (1) No fluid pressure applied.

      (2) Localized hydrostatic pressure applied at the punch-sheet interface, using a vinyl sheet.

      (3) Fluid pressure applied to one surface of the sheet metal:

         a. Constant fluid pressure.

         b. Varying fluid pressure.

   B. Deep Drawing:

      (1) No fluid pressure applied.

II. Numerical Studies:

A. Studying several important issues related to in establishing the reliability of the FEA model that could be used for hydroforming simulation. These include:

   (1) Material modeling.

   (2) Constitutive model effects: Using the isotropic von-Mises yield function versus Barlat's 1996 anisotropic yield function.

   (3) Geometrical effects: The effects of forming a square blanks vs. a round blank and its effect on wrinkling behavior in the deep drawing experiments.

   (4) Element formulation (integration schemes) effects: The effects of using a fully integrated integration scheme vs. reduced integration schemes, e.g. Hughes-Liu, Belytechko-Tsay, on the accuracy of the model.

B. Simulating sheet hydroforming process, with the explicit dynamic finite element analysis (FEA) code LS-Dyna 3D, using the above experimental conditions.

C. The FEA code is used to simulate the deep drawing case with fluid pressure to extract the lower limit of the optimal pressure curve (Figure 2).

In the following section, the experimental works will be described, some results will be presented, and some important issues encountered will be discussed. For comparison, all experimental results will be presented side by side with the numerical analysis results in chapter 6.

4.3. Experimental Work

4.3.1 Pure Stretching Experiments, No Fluid Pressure Applied:

For the experiments conducted under pure stretching conditions without fluid pressure, the 1 mm thick, square blank (178mm x 178mm) was placed over the draw bead and clamped with a blank holding force (BHF) of approximately 267 kN. To ensure that no draw-in occurs, several tests were conducted where the edge of the sheet on either side of the draw bead were marked with a thin pencil before forming. After the forming, the location of these lines with respect to the draw bead was checked for any possible movements. In all the tests it was verified that the marked lines did not move at all, confirming the pure stretching condition of the sheet. After clamping the sheet, the punch was moved against the sheet until rupture of the material occurred. Using special software, several important readouts were recorded against time. These were the punch and clamp travel, also the clamp and punch loads. The rupture point was detected when the punch load dropped sharply at the point of rupture. Figure 10 shows a deformed part. The rupture point was recorded at a depth of 24.6mm (0.9692 in).

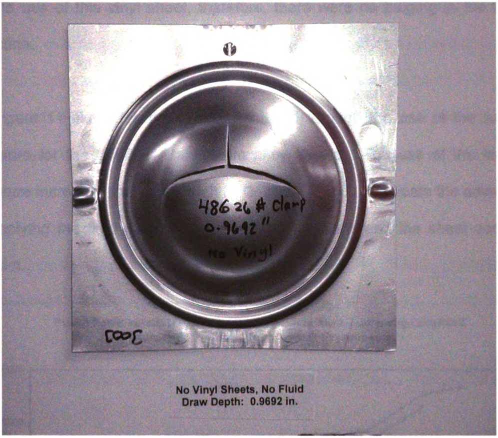

Figure 10. Pure stretching of the AA3003-H14 sheet metal without fluid pressure.

4.3.2 Localized Hydrostatic Pressure Applied Using Vinyl Sheet:

In an attempt to explore different design ideas, the process was conducted using a thin vinyl sheet in place of the counteracting fluid. The vinyl material was a stiff material that was also stretchable. By placing this material over the sheet metal the effect of a localized hydrostatic pressure was simulated. As the punch moved into the sheet metal the vinyl counteracted the motion and added a pressure at the location of the sheet metal that was in contact with the punch. Due to its stiffness, the unsupported regions of the sheet metal were unaffected by the use of this vinyl sheet, therefore, there were no bulging in the reverse direction.

Figure 11 illustrates the results achieved through the use of the localized pressure for the 3003-H14 aluminum alloy sheets. The use of the localized pressure increased the draw depth by 3–10%. This may indicate the advantages of applying the fluid pressure where only the punch and the sheet come into contact.

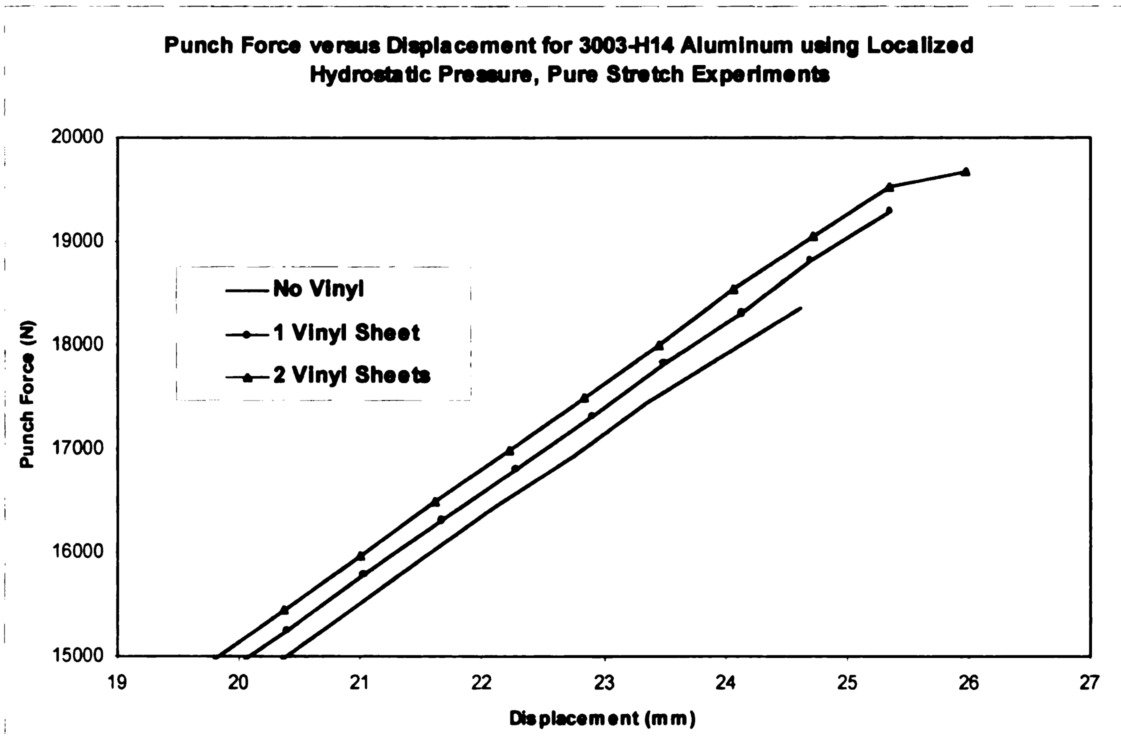

Figure 11. Force versus displacement for 3003-H14 aluminum sheets with a hydrostatic force applied by vinyl sheets, pure stretch experiments.

By coating the punch with a thin layer of grease prior to forming, the surface area that contacts the vinyl could be quantified. Using this value an approximate equivalent pressure could be calculated using the relationship between the forces applied by the punch and the surface area (P=F/A). For the single vinyl sheet this was calculated as 148 kPa (21.5 psi), while the use of two vinyl sheets was calculated as being equivalent to applying a fluid pressure of 159 kPa (23 psi). Since the vinyl sheet had no effect on the sheet metal that was not in contact with the punch then it was concluded that this vinyl sheet was applying an equivalent fluid pressure locally instead of globally. Therefore, based on the increased draw depths achieved using a relatively low localized pressure, it could be assumed that increases in the fluid pressure, applied locally, should result in better formability of the sheet metals.

4.3.3 Pure Stretching, Constant Fluid Pressure Applied to Topside of the Sheet:

In this experimental setup, after the blank was clamped as motioned previously, the fluid chamber was filled using a small pump and then given an initial pressure of 2758 kPa (400 psi). Figure 12(a) shows the measured constant pressure used in the experiment. As the pressure within the chamber increased, the sheet bulged in reverse direction towards the punch (away from the fluid chamber) prior to the punch beginning its movement into the sheet metal. This bulging, schematically illustrated in Figure 13, created a strain concentration around the rigid die corner, which had a radius of curvature of 6 mm (0.24 in). With the constant fluid pressures above 3448 kPa (500 psi), the material sheared off at the sheet/die corner interface prior to the punch moving into the fluid chamber.

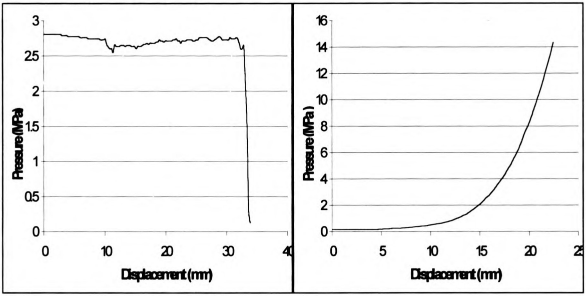

(a) (b)

Figure 12. Experimental fluid pressure curves, (a) constant and (b) varying fluid pressure profiles.

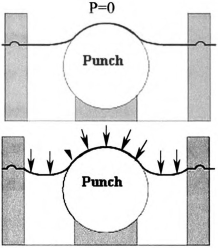

Figure 13. Example of material sag in unsupported regions when a constant fluid pressure is applied on the topside of the draw blank material (gap exaggerated to illustrate effect).

Maintaining the fluid pressure below the critical 3448 kPa level led to increased draw depths for the 3003-H14 aluminum alloy as illustrated in Figure

14. Experiments were conducted at several pressure levels in order to quantify the upper bound of the fluid pressure/punch stroke diagram for the constant fluid pressure, pure stretch experiments. Maintaining a constant fluid pressure allowed for an impressive increase in the forming depth of 12-31% over parts that were formed without the resisting fluid (i.e., conventional stamping). This improved formability could be attributed to several factors, but is mostly caused by changes in the boundary conditions. One explanation could be that when the sheet bulges in one direction (e.g., toward the punch) followed by a deformation in the opposite direction, the in-plane and bending strains in the sheet will reverse, causing the sheet to work harden. Depending on the amount of the work hardening, the resistance of the sheet to failure will increase. Also, this reverse bending and stretching causes the entire sheet metal in the die cavity to deform plastically and therefore strain localization over the punch surface will be delayed. Another reason for the improved formability could be that when the initial bulging occurs it creates more material in the die cavity to be deformed by the punch (see Figure 13), in comparison with conventional stamping where the length of the sheet metal in the die cavity is shorter (see Figure 1.1).

As will be discussed in the discussion of results section, Chapter 6, this improved draw-depth was also observed in the numerical modeling.

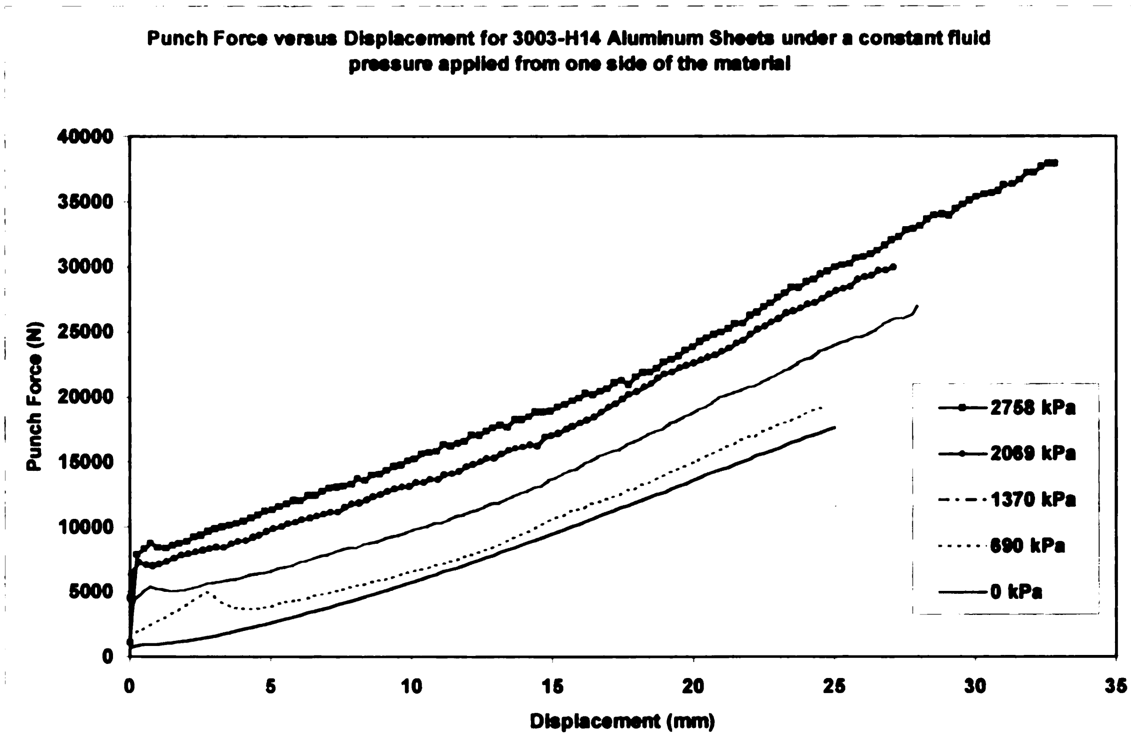

Figure 14. Punch force versus displacement for 3003-H14 Aluminum alloy sheet metal using a constant fluid pressure applied form one side of the draw blank, pure stretch experiments.

4.3.4 Varying Fluid Pressure Applied to One-Side of the Sheet:

The goal of the varying fluid pressure experiments was to try to delay the occurrence of the strain localization by gradually increasing the pressure in the fluid chamber (see Figure 12(b)) as the punch deformed the sheet, while maintaining an upper pressure bound of 2758 kPa (400 psi). The main obstacle with these experiments was the control of the fluid pressure. At times, the fluid pressure was found to spike at levels that were over twice the set boundary level of 2758 kPa. Though these spikes lasted for only milliseconds they were long enough to impart significant stress concentrations to the material. Several experiments were successfully run with aluminum sheet metals. Parts that were being formed using an applied varying hydrostatic fluid pressure were rupturing at shallower draw depths than those parts formed without any resisting fluid pressure. These premature ruptures were primarily due to excessive thinning of the sheet metal, caused by the extra tension created by the applied pressure. The higher the fluid pressure was, the earlier the sheet failed in these experiments.

4.3.5 Deep Drawing Experiments, No Fluid Pressure Applied:

The objectives behind these experiments were twofold. The first objective was to study the wrinkling behavior of the sheet metals, then using the hydroforming process to try to reduce and iron out these wrinkles. From these experiments the lower limit of the fluid pressure profile as it relates to the punch stroke, Figure 2, can be established. The second objective relates to the accuracy of the numerical modeling. Wrinkling is a very complex material behavior that is not easily captured by the FEA method [1, 24, 26, 29]. In order to achieve the desired accuracy and establish confidence in the numerical analysis method, it had to be shown that the numerical model could capture wrinkling behavior with good accuracy.

In the deep drawing experiments, a flat-type blank holder, i.e. without drawbead, was used to allow the material to flow easily into the die chamber. Two types of blank holding method were then tested. They were:

1. The Blank Holder Force (BHF) type control. In this method the blank holder was given a much lower blank holding force than the one used in the pure stretch. A BHF between 2kN – 6kN (450lbf – 1349lbf) was used.
2. The Blank Holder Displacement Control (BHDC). In this method, the lower blank holder was held at a desired distance away from the upper blank holder, e.g. 4 mm (0.16 in).

In both of these two blank holding methods, round blanks were used. The sheet was first lubricated and placed under the blank holder. The punch was then moved up against the sheet, pushing it into the upper chamber of the die. As the punch moved further into the upper die, more material also was drawn into the upper die cavity. Because of the material and geometrical effects, wrinkles formed both underneath the blank holder (if the blank holding forces were low enough < 2 kN) and in the unsupported region of the blank (between the punch and the die cavity).

Depending on the material used, when blank holding forces higher than 2 kN for the 3003-H14, and higher than 4 kN for the 6111-T4 were used, no wrinkles formed underneath the blank holder. In these cases, internal forces generated were lower than the critical compressive (internal) forces needed to wrinkle the sheets. Therefore, the higher blank holding forces prevented, and ironed, any wrinkles from forming underneath the blank holder.

Figure 15 shows the result of using the 101.6mm (4in) hemispherical punch and the BHDC blank holder control scheme to form the part. The distance between the lower and upper blank holder was kept at 4mm (0.16in). Figure 16 shows the same result when forming the sheet with a 76.2mm (3in) diameter hemispherical punch using the BHF control type. The blank holder force used was 2KN (450lbf).

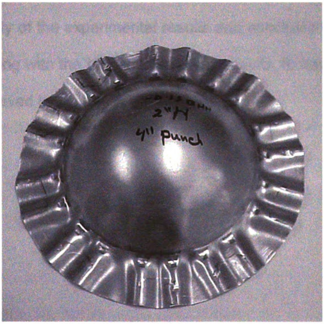

Figure 15. Deep drawing experimental result using the 101.6mm (4 in) punch with 4mm (0.16 in) blank holder displacement control (AA6111-T4).

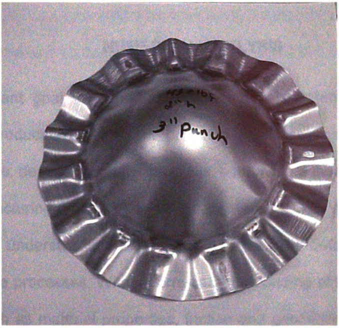

Figure 16. Deep drawing experiment using the 76.4mm (3in) punch with 2 kN (450lbf) BHF (AA6111-T4).

The majority of the experimental results and conclusions will be presented in Chapter 6, along with the numerical analysis results, to have a better view of the accuracy achieved in the numerical analysis.

Chapter 5

NUMERICAL ANALYSIS

An important goal in manufacturing research is determining the optimum method of production of efficient products with less cost. The optimization criterion varies, depending on the products, but having a thorough understanding of the manufacturing processes is an essential step. Sheet metal forming design requires the understanding of the fundamentals of deformation mechanics involved in the processes. Without proper understanding of the effect of different variables such as material properties, friction and geometry the design process would be difficult, time consuming, and expensive. Also it would not be possible to predict and prevent defects form occurring until it is too late.

Failure modes such as necking, wrinkling and springback may occur in sheet metal forming process. The automotive industry in recent years has seen more use of very thin high strength materials in which defects like folding and wrinkling occur more often. The finite element method (FEM) gives an advantage in predicting such defects, before the real stamping operation takes place [31].

An important goal of this research was to develop a rigorous finite element analysis (FEA) model that could be used to achieve a better understanding of the deformation of the sheet metal during the forming process, and as a predictive tool for several failure modes to reduce the number of costly experimental verification tests. Commercial FEA codes are robust enough that they could be used with confidence as a predictive tool, provided that the correct description of complex geometrical contact, force and displacement boundary conditions and, material model... etc, are incorporated. The importance of the correct parameter description increases even more when material anisotropy is considered. The FEA model would be used to aid in the prediction of the final part geometry (design process), compare results against experimental data and to reduce the amount of trial and error associated with the experimental aspect of the work.

For the stamp hydroforming process the numerical study was performed using the explicit finite element code, LS-Dyna 3D. In the following a general description of the FEA code built for this analysis will be discussed. Several important issues in establishing the FEA code will be discussed. After that a comprehensive comparison between experimental and numerical results will be discussed in Chapter 6.

5.1. FEA Code Setup

LS-Dyna↑ is a general-purpose transient dynamic finite element program capable of simulating complex real world programs [34]. Altiar's Hypermesh↑ pre-processor was used to create the finite element input deck for LS-Dyna.

A 3-D geometrical description of the model was built using Unigraphics® then imported as IGES files. The file was then imported into Hypermesh® and used to create the mesh, assigning the boundary conditions and to build the LS-Dyna input deck for the analysis. Manual editing of the input deck was needed since Hypermesh® does not support all LS-Dyna input cards.

Two types of finite element models were used for this study: a quarter-model and a full model. Figure 17 shows the full 3-D model, while Figure 18 shows the quarter model. Two types of element formulation were used: Shell and Solid elements. The majority of the analysis was carried out with the shell element formulation.

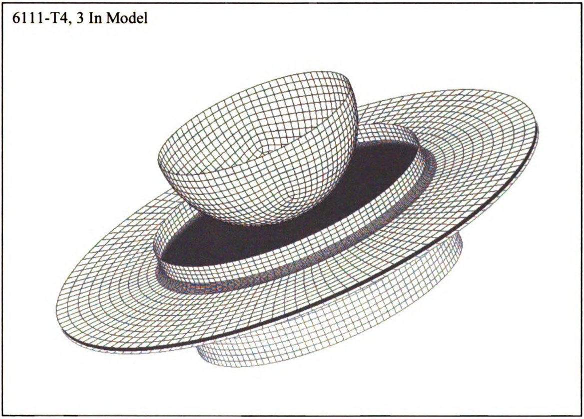

Figure 17. LS-Dyna Full 3-D model created for stamp hydroforming process with a hemispherical punch, using square blank.

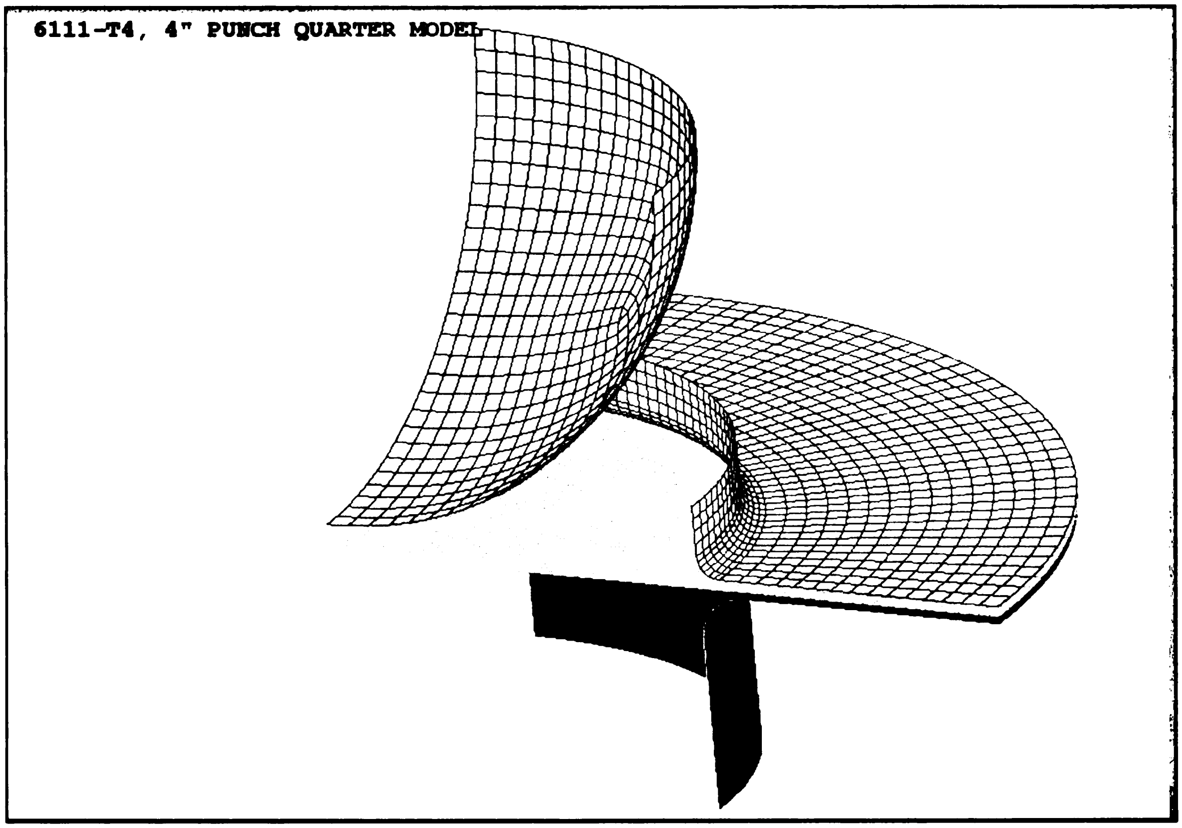

Figure 18. Quarter-model of the hydroforming process using a hemispherical punch with a round blank.

The full size finite element model, Figure 17, used approximately 10500 four-noded shell elements, while the quarter-model, Figure 18, used 4600 elements. Another quarter model, where the sheet metal is modeled using solid elements, was also built. The solid model consisted of 40500 quad elements; with the sheet having 5 layers and one integration point per each through-thickness layer.

The punch, die, and the blank-holder were created using rigid material (Material 20 in LS-Dyna) with one integration point through the thickness to reduce the processing time.

5.2. Important Issues Affecting FEA Accuracy

During the development process of the FEA model, several important issues were encountered that had an effect on the accuracy of the modeling capabilities. These will be presented next.

5.2.1 Material Modeling:

The first material to be used in the experiments was the AA3003-H14. At that time, and after an extensive search in the literature, no specific constitutive material model data for this material was found. The first material model chosen for the analysis was Material-Type#18 in LS-Dyna: *MAT_POWER_LAW_PLASTICITY. This is an isotropic plasticity model with rate effects which uses the Hollomon power law hardening rule as follows:

$$\sigma = k\varepsilon^{n} \tag{5.1}$$

Where "k" is the strength coefficient, and "n" is the work hardening exponent.

Since no mechanical properties were available for the 3003-H14 in the literature, a uniaxial tensile test was carried out for the material. From this test, using a simple curve fitting technique, the values of k and n were found as reported in Table 1.

	σ_y Yield Stress	E Young's Modulus	ν (Poisson Ratio)
3003-H14 (Assumed initial values)	150.6 MPa	69 GPa	0.33
	k	n	Thickness (t)
	538.43 MPa	0.325	1 mm

Table 1. AA3003-H14 assumed initial properties.

Initial comparison between the numerical analysis and the experimental data revealed that the values of "k" and "n" obtained from a simple curve fitting technique were not correct. Using the above values, compared to experiments, the numerical analysis predicted much higher punch forces and draw depths, before material failure. Figure 19 shows the comparison between the predicted force-displacement and the experimentally measured values. It is obvious that the two sets of data do not match. Also, the rupture point or failure was over predicted compared to the experiments (24.4mm (0.96 in) experimental vs. 30.5mm (1.2 in) numerical).

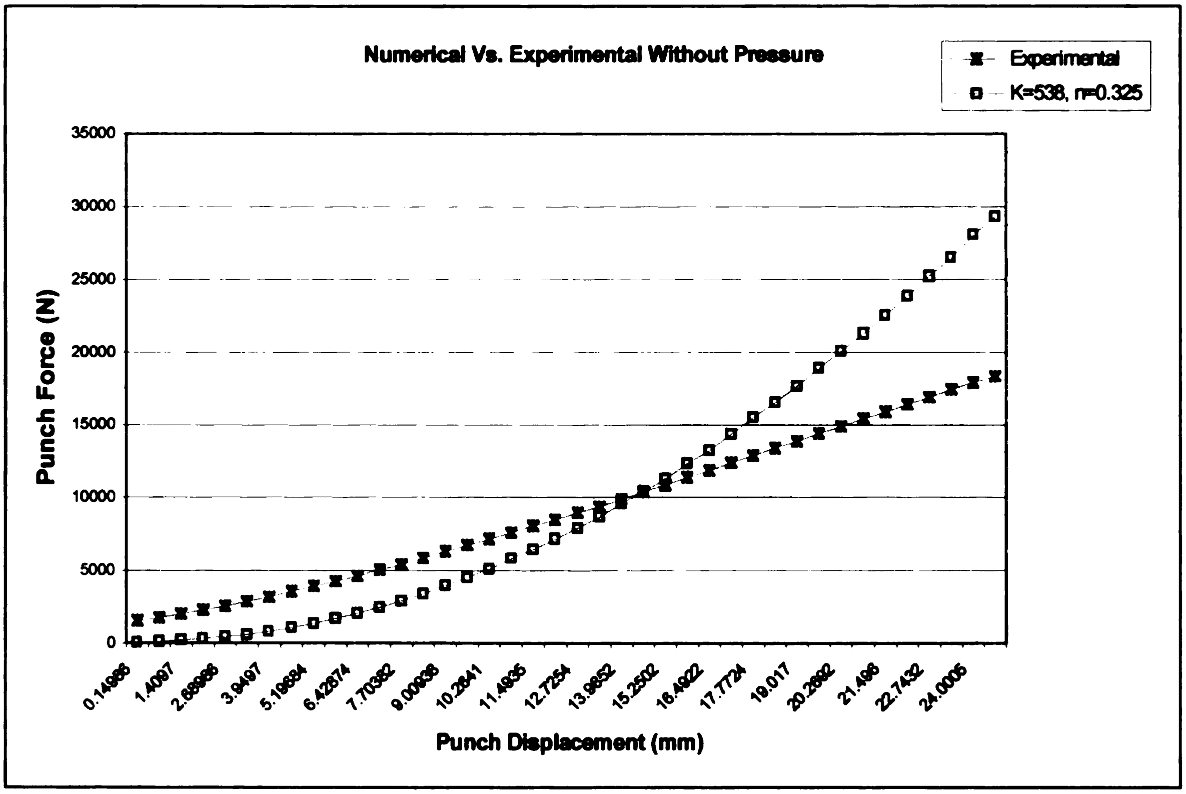

Figure 19. Punch force versus punch displacement, using k and n values from Table 1 for AA3003-H14.

To solve this problem, a different approach was used to calculate "k" and "n" values from the uniaxial tensile test data. In the second technique, the Considere criterion for failure was employed to calculate the new vales for "k" and "n". The method is as follows:

Starting from the Considere criterion:

$$\frac{d\sigma}{d\varepsilon} = \sigma \tag{5.2}$$

and using the power-law relationship:

$$\sigma = k\varepsilon^{n} \tag{5.3}$$

we obtain:

$$\frac{d\sigma}{d\varepsilon} = nk\varepsilon^{n-1} = \sigma = k\varepsilon^{n} \tag{5.4}$$

From (5.4), the following relationship between the maximum strain and n can be found:

$$\frac{n}{\varepsilon} = 1 \tag{5.5}$$

The true stress at the maximum load is also known from [37]:

$$S_u = k\left(\frac{n}{e}\right)^{n} \tag{5.6}$$

where e = 2.7183 is the base of the natural logarithm.

By utilizing equations (5.3) and (5.6) and assuming that $\sigma = \sigma_y$ when $\varepsilon = 0.002$ it is possible to obtain the following implicit equations for parameter "n":

$$n = \frac{ln(\sigma_y) - ln(S_u)}{ln(0.002) + ln(e) - ln(n)} \tag{5.7}$$

The above equation could be solved for n, iteratively, for known values of the ultimate stress, S_u, and the yield stress, σ_y, of the material. From the uniaxial tensile test for AA3003-H14, a value of $S_u = 166.78$ Mpa was determined at the ultimate load. Using the 0.2% offset condition, the yield stress was also calculated to be σ_y=150.42 Mpa.

By substituting these values into equation (5.7) and solving iteratively using MS-Excel, the following value for the hardening coefficient "n" was obtained:

$$n = 0.0476 \quad (5.8)$$

The strength coefficient "k" was then calculated from equation (5.3) to be:

$$k = 202.2 \text{ Mpa} \quad (5.9)$$

Figure 20 shows the true stress-strain curve for the material and the two curves representing the two different sets of "k" and "n" values. The figure clearly shows that the calculated values using the second method produces a much more accurate and realistic representation of the behavior of the AA3003-H14 aluminum sheet material.

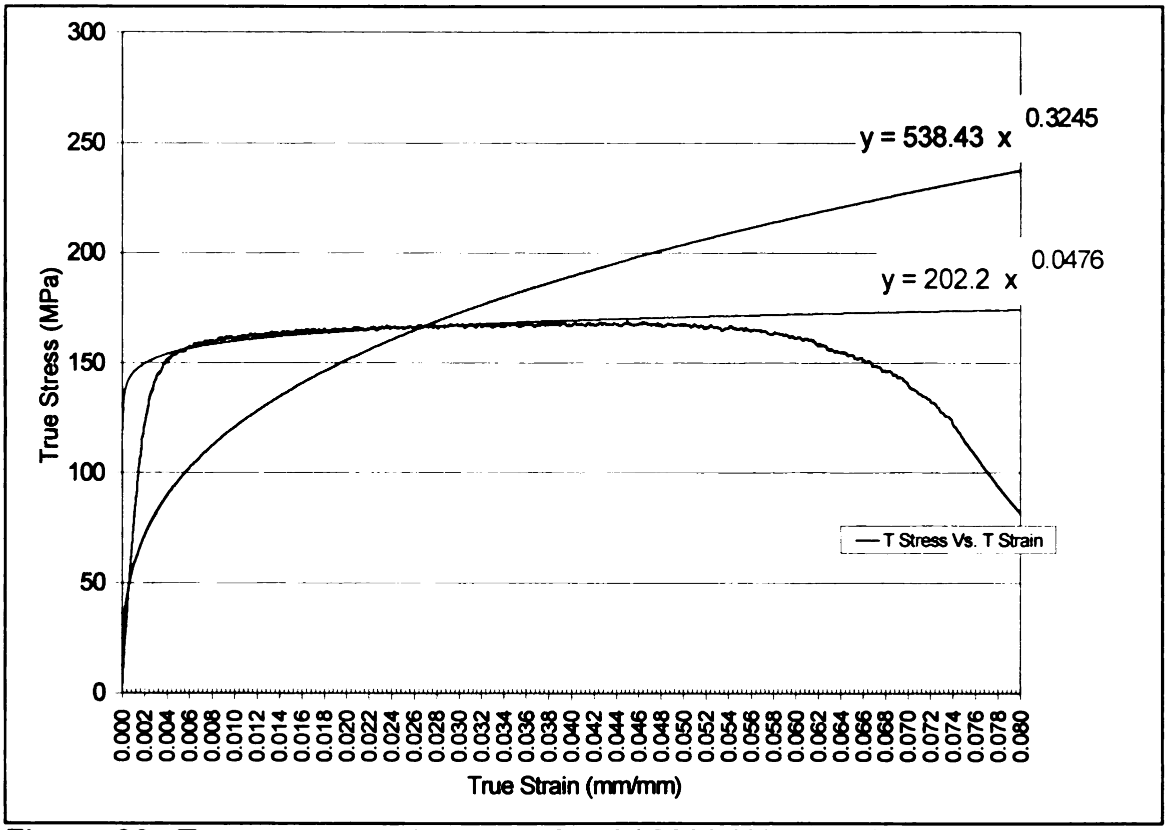

Figure 20. True stress-strain curve for AA3003-H14-aluminum alloy sheet is compared with curves plotted using (k=538.43 MPa, n=0.35) and (k=202.2 MPa, n=0.0476) values.

Using the new values for "k" and "n", as shown in Table 2, the numerical analysis was repeated for the forming process. Figure 21 shows the comparison between the predicted punch force vs. punch displacement and the experimentally measured values. From the figure we notice that the failure point (drop) is also predicted correctly by the numerical analysis.

	σ_y Yield Stress	E Young's Modulus	ν (Poisson Ratio)
3003-H14 (Assumed initial values)	150.6 MPa	69 GPa	0.32
	k	n	Thickness (t)
	202.2 MPa	0.0476	1 mm

Table 2. AA3003-H14 calculated properties.

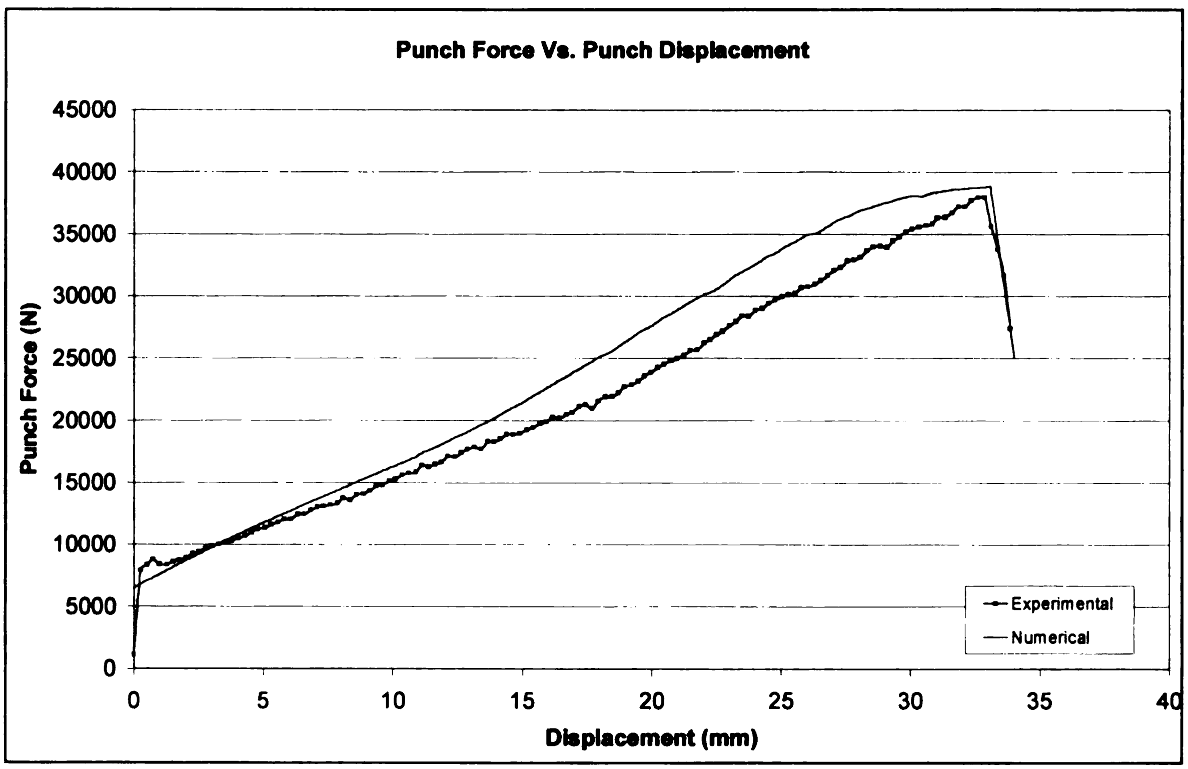

Figure 21. Predicted and measured punch force vs. punch displacement for calculated values of "k" and "n" (from Table 2) for AA3003-H14.

Although the previous model captured the hardening behavior of the material, it did not capture the anisotropic characteristics of the aluminum sheet. Therefore, another material model was employed to simulate the anisotropic behavior of the material. Material #36 in LS-Dyna: *MAT_3-PARAMETER_BARLAT. The material properties used in this simulation are shown in Table 3.

AA3003-H14	σ_y (Yield Stress)	E	ν (Poisson Ratio)
	150.6 MPa	69 GPa	0.33
	k	n	Thickness (T)
	202.2 MPa	0.0476	1 mm
	R_{00}	R_{45}	R_{90}
	0.500	0.550	0.650

Table 3. Material properties for 3003-H14 using Barlat model.

The second material used in the experiments was the AA6111-T4. Another anisotropic material model was chosen for modeling this material, Material-Type# 33 in Ls-Dyna: *MAT_BARLAT_YLD96. Barlat et al. [38] developed this yield function to model the anisotropic behavior of sheet metals, especially aluminum (this model will be described more thoroughly later). The material properties used in the analysis for the AA6111-T4 was supplied by Dr. Barlat form ALCOA (Aluminum Company of America), as shown in Table 4.

	σ_y (Yield Stress)	E	ν (Poisson Ratio)	Thickness (t)	Coulomb Friction	
AA6111-T4	180.0 MPa	71 GPa	0.33	1 mm	0.01	
	c1	c2	c3	α_1	α_2	α_3
	0.9392	0.8512	1.0631	2.45	2.35	0.68

Table 4. AA6111-T4 Material prosperities (From ALCOA).

5.2.2 Constitutive Model Effects:

Constitutive model effects refer to the type of constitutive equations (material representation) used in the numerical analysis. As mentioned earlier, two types of constitutive models were used: isotropic and anisotropic. The isotropic material model was used initially since anisotropic material properties were unavailable. Later in the study, it was noticed that the isotropic model fails to capture the true material behavior, especially wrinkling that were occurring in the experiments. Therefore, the anisotropic material model was used.

Figure 22 shows the draw in result using the AA3003-H14 material. It is clear from the figure that the material is anisotropic and wrinkling only occurs along the rolling direction of the sheet. Initial numerical analysis using the isotropic material model (material #18 in LS-Dyna: *MAT_POWER_LAW_PLASTICITY) is shown in Figure 23. From this figure the isotropic nature of wrinkling is clear, since the wrinkles occurs along both axes of the material.

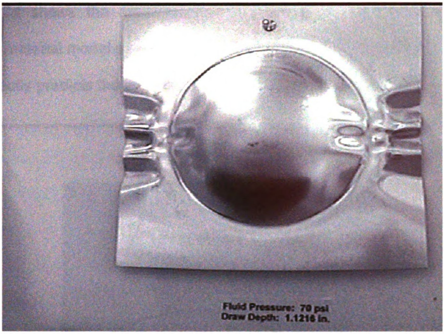

Figure 22. Experimental results for the draw-in case (AA3003-H14).

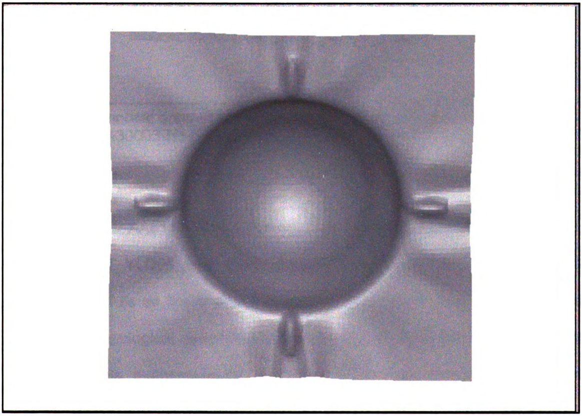

Figure 23. Numerical draw-in simulation using the isotropic material model in LS-Dyna (AA30003-H14, 4 in punch).

Figure 24 shows the resulting deformed shape of the sheet using the anisotropic material model properties (Table 3). It is clear that now the numerical model correctly predicts the wrinkling behavior of the aluminum sheet.

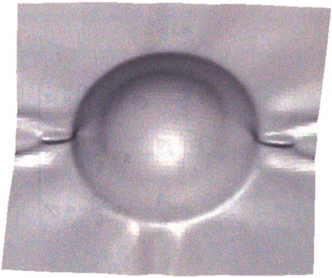

Figure 24. Numerical draw-in simulation using Barlat's anisotropic material model in LS-Dyna (AA30003-H14, 4 in punch).

For the AA6111-T4 material, a better constitutive model, *MAT_BARLAT_YLD96 was used. Barlat et al. (1997) [38] presented this material model as an improvement to their YLD-91 model. The model is based on a phenomenological description of the material. To represent the behavior of these materials mathematically, a yield function was proposed, and then generalized to include the most general stress tensor with six components as shown in the following equations:

$$\Phi = \alpha_1 | S_2 - S_3 |^a + \alpha_2 | S_3 - S_1 |^a + \alpha_3 | S_1 - S_2 |^a = 2\bar{\sigma}^a \qquad (5.10)$$

where,

$$S = L\sigma \qquad (5.11)$$

$$\left\{ \begin{array}{l} s_1 = \frac{c_3 + c_2}{3}\sigma_x \quad -\frac{c_3}{3}\sigma_y \quad -\frac{c_2}{3}\sigma_z \\ s_2 = -\frac{c_3}{3}\sigma_x \quad +\frac{c_3 + c_1}{3}\sigma_y \quad -\frac{c_1}{3}\sigma_z \\ s_3 = -\frac{c_2}{3}\sigma_x \quad -\frac{c_1}{3}\sigma_y \quad +\frac{c_1 + c_2}{3}\sigma_z \end{array} \right\} \qquad (5.12)$$

and,

$$\alpha_k = \alpha_x p_{1k}^2 + \alpha_y p_{2k}^2 + \alpha_z p_{3k}^2 \qquad (5.13)$$

Where c_1, c_2, c_3, α_1, α_2, α_3 are material coefficients that describe anisotropy. ***P*** is the transformation matrix from the principal axes of anisotropy (**x**, **y** and **z**) to the principal axes of **s** (P_{ij} is the *i-th* component of the *j-th* unit principal vector $\boldsymbol{P}_j$). With this it is possible to increase the pure shear yield stress without increasing the other plane strain yield stresses.

The material coefficients c_1, c_2, c_3, α_1, α_2, α_3 for AA6111-T4, supplied by Dr. Barlat, are in Table 4.

Figure 25, illustrates the importance of choosing a material specific constitutive model. In Figure 25(a) the simulation was run using the 76 mm (3 in) punch with an isotropic material model. Figure 25(b) was the same simulation using Barlat's 1996 yield function. The effect of the anisotropy on wrinkling prediction is clearly visible, especially around the clamped region of the part. Compared to the experimental results the ability of the isotropic model to predict wrinkles is limited and inaccurate whereas the anisotropic model much more closely resembles the parts being formed experimentally.

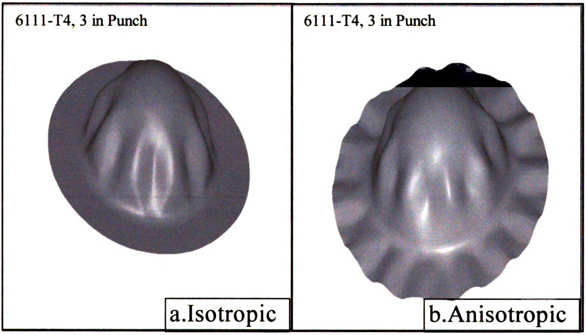

Figure 25. Isotropic vs. anisotropic material model.

<u>5.2.3 Geometrical Effects:</u>

Wrinkling is a complex phenomenon that is affected by many factors such as geometrical, material properties and boundary conditions. Figure 26 shows the geometrical effects of using a square blank versus a round blank on the formation of wrinkles. In the square blank, wrinkles do not form underneath the blank holder, where the part reaches its failure point due to rupturing before wrinkles form, while for the round blank the wrinkle occurrence is apparent. These numerical results were verified experimentally for both blank types.

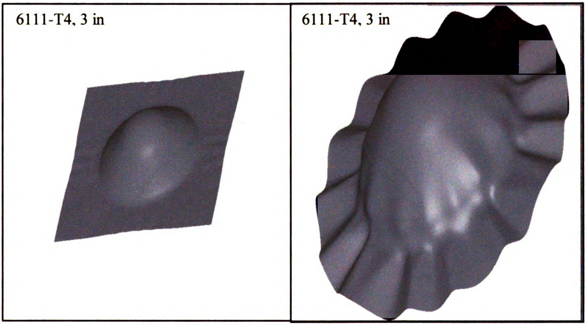

Figure 26. Geometrical effects on wrinkling.

5.2.4 Element Formulation (Integration Scheme) Effects:

The computational speed of the numerical analysis depends on many factors, but one common simplification method in shell elements is to use the reduced integration schemes versus the fully integrated schemes. In this analysis two types of element formulations were used for the blank: the Hughes-Liu shell element formulation (ELEFORM #1), and the fully integrated shell element (ELEFORM#16). Both schemes used 7 integration points through the thickness.

The results showed that the calculation time doubled when using the full integration scheme compared to the other formulation, but a significant improvement in accuracy was achieved when comparing numerical results to experimental ones. This is shown in Figure 27.

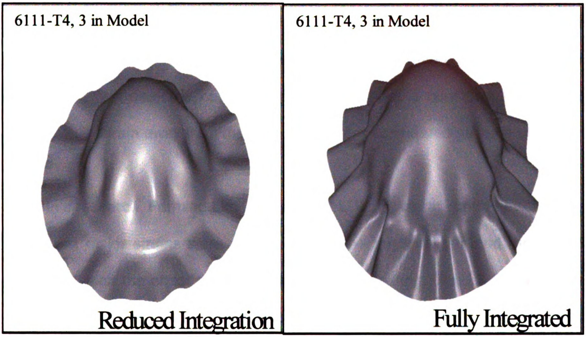

Figure 27. Reduced integration vs. full integration.

So, while the reduced integration scheme is accurate and computationally efficient for predicting failure due to rupture, a full integration scheme is recommended for accurate wrinkling prediction. All subsequent numerical analysis involving wrinkling was conducted using Barlat's 1996 yield function with a full-integration scheme and round blank shapes, while in the analysis of tearing the reduced integration scheme was used.

5.3. Failure Criteria

In sheet-forming operations, the deformation is characterized by biaxial stretching [37]. Failure in stretching operations normally occurs by the development of a sharp localized neck on the surface. By measuring minor and major strains in a specimen during deformation and plotting them, a Forming Limit Diagram (FLD) can be constructed. In sheet forming, the value of the measured strain near the necked region of the sheet is considered as "failed strain", while strain away from the necked region is considered as "safe strain".

In this research, Forming Limit Diagrams (FLD) displaying contour plots of the minor and major strains were used to determine the locations and the punch height at which the sheet metal would fail due to tearing. The LS-Dyna code's new post-processor has the ability to calculate the FLD plot, using the thickness and the "n" values of the sheet material. Color codes are used to distinguish several areas of the sheet. Areas that failed are characterized as "red".

In the next chapter, the results of the experimental and numerical analysis are presented.

Chapter 6

DISCUSSION OF RESULTS: EXPERIMENTAL VERSUS NUMERICAL

In the following sections, results of the experimental and numerical analysis will be presented.

6.1 Stamp Forming

6.1.1 Pure Stretch, No Fluid Pressure Applied:

In the no pressure modeling, the punch was given a trapezoidal velocity profile to fit the curve shown in Figure 28.

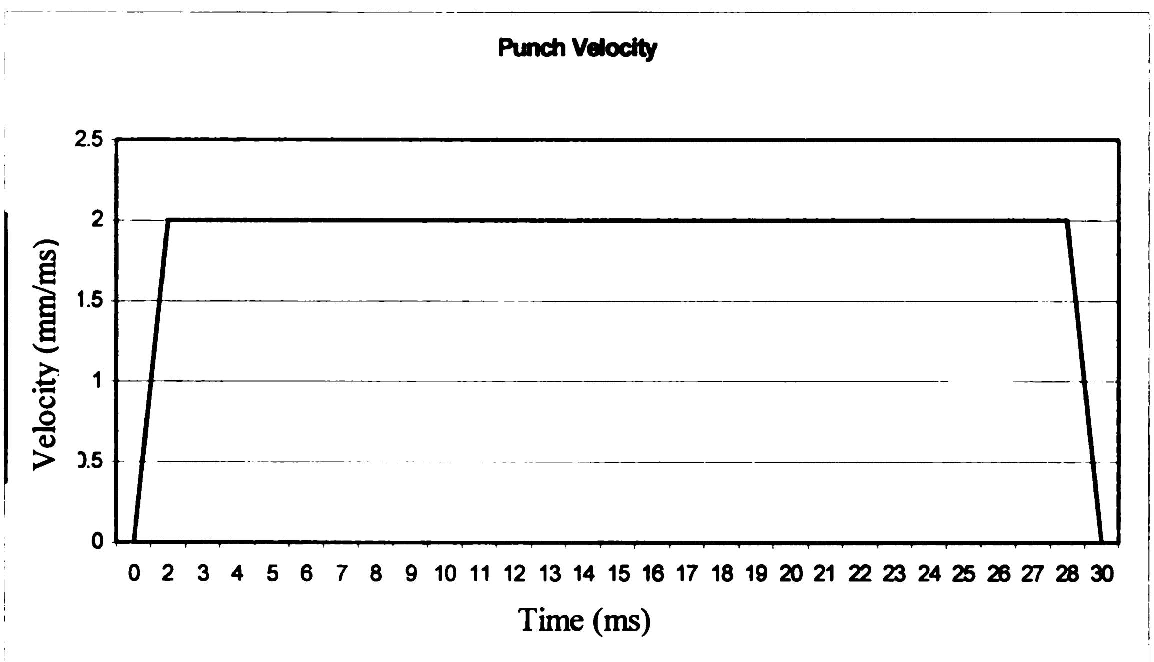

Figure 28. Punch velocity used for the finite element simulation.

The results of both the FLD-numerical and experimental analysis for sheet stamping without pressure are shown in Figure 29. The experimental result shows that the material failure occurs at a stamping depth of 24.6mm (0.969 in). For the numerical result the FLD contour plot was used to determine the failure point. From the plot it was determined that the initial failure would occur around the center of the sheet at a punch depth of 23.6mm (0.93 in). This represents a 4% discrepancy between the experimental and the numerical results, which for all practical purposes is acceptable.

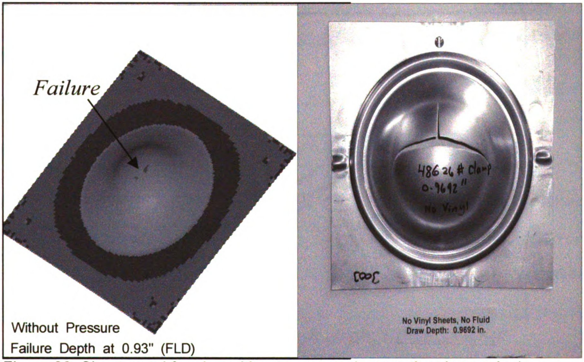

Figure 29. Sheet metal forming without pressure (conventional stamping).

Figure 30 shows the punch force-displacement for the experimental and numerical analysis up to the initial failure. It was noted that the experimental punch force was slightly higher than the numerical predictions. The load cell used in the experimental investigations has a capacity of 70,000 lbf with an error of 1%. If an error of less than 0.5% is assumed (>350 lbf or 1500 N), and this error is subtracted from the experimental data, then we get the results shown in Figure 30 (Adjusted Force) for the AA3003-H14, which matches the numerical predictions very well. Figure 31 shows the results for the AA6111-T4 aluminum sheet.

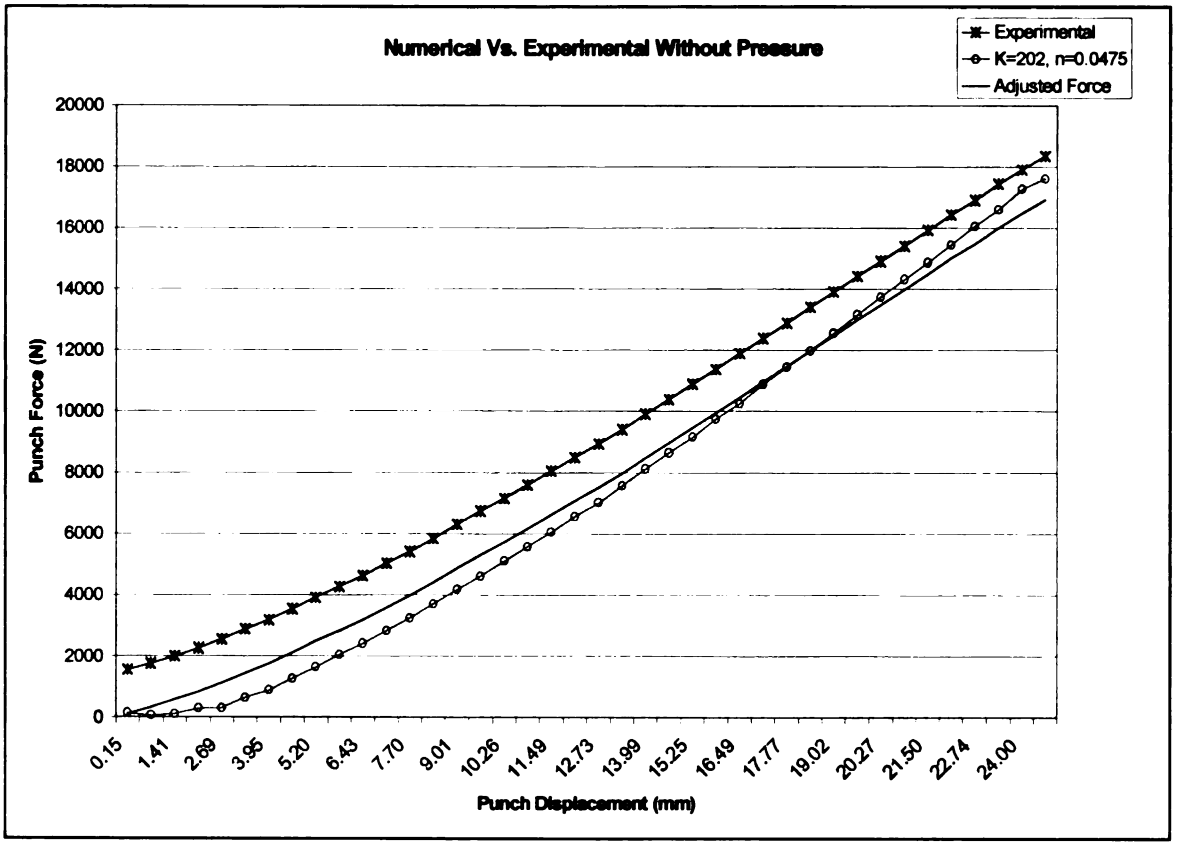

Figure 30. Predicted and measured punch force vs. punch displacement curve for AA3003-H14.

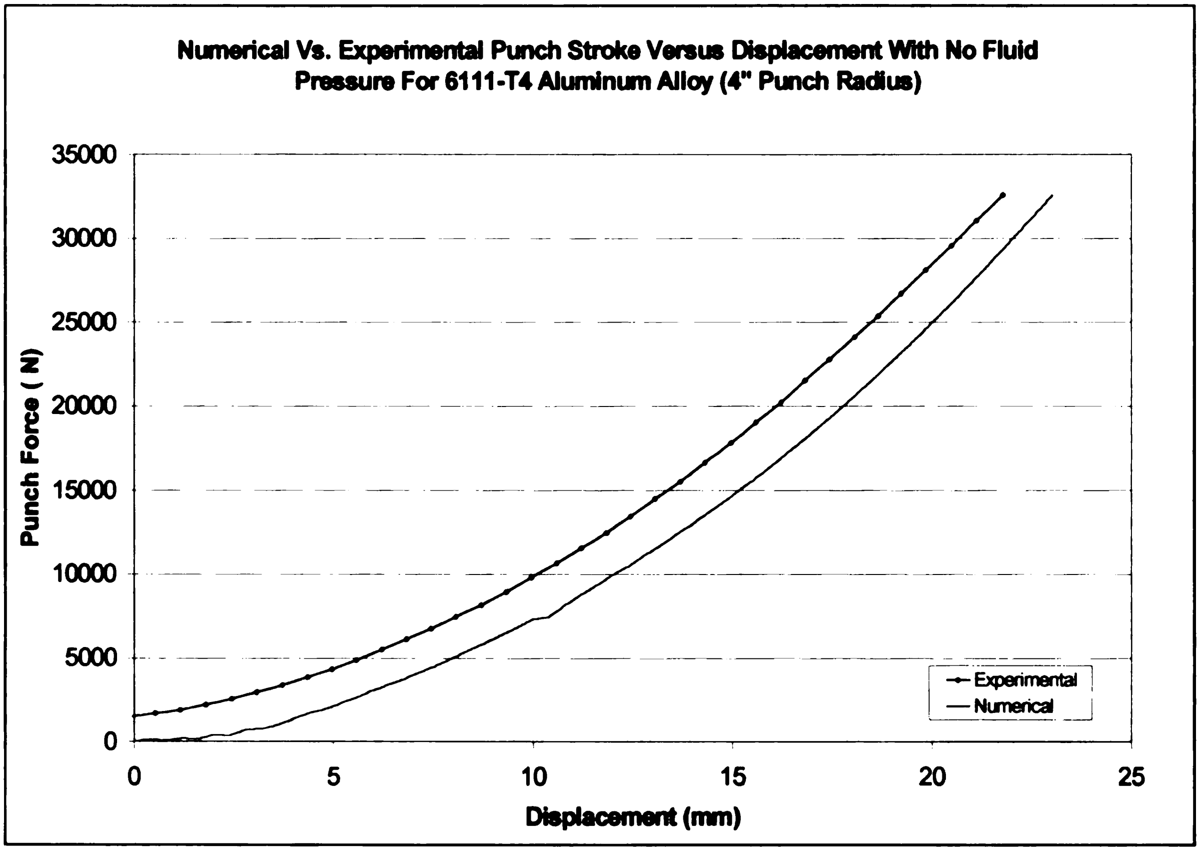

Figure 31. Predicted and measured punch force vs. punch displacement curve for AA6111-T4. Without fluid pressure.

6.1.2 Pure Stretch, Constant Fluid Pressure Applied to Topside of Sheet:

In the experimental procedure, the punch was first brought up until it touched the bottom of the sheet and then stopped. Then, the fluid pressure was raised to a desired value and kept constant at that level before the punch was allowed to move up to deform the sheet. To simulate this in the numerical model, the punch was controlled by the displacement profile shown in Figure 32.

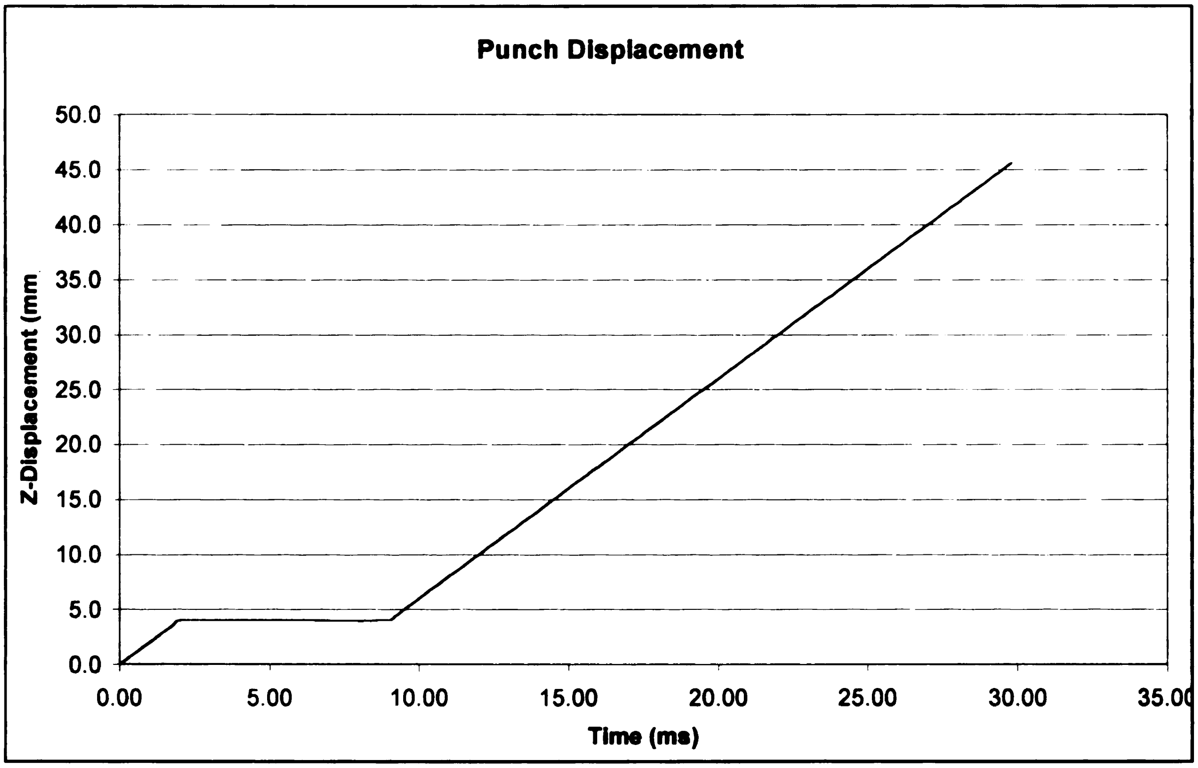

Figure 32. Punch displacement profile for one-sided hydroforming simulation.

The constant pressure used in the simulation was ramped up over a time period of 7-ms. Similar to the experiments, at the constant pressure level of 3448 kPa (500 psi), the numerical model correctly predicted that the sheet would fail, before the punch moves, along its corner radii due to strain localization as shown in Figure 33.

In the experiments with a constant fluid pressure of 2758 kPa (400 psi) it was found that the sheet sometimes fails along the corner radii, as shown in Figure 34, soon after the punch starts deforming the sheet. After further investigation, it was found that due to an initial controller-regulator problem in the experimental setup the fluid pressure was not being kept at the desired constant level of 2758 kPa (400 psi), but instead was ramping up from 2758 kPa (400 psi) to 7000 kPa (1000 psi).

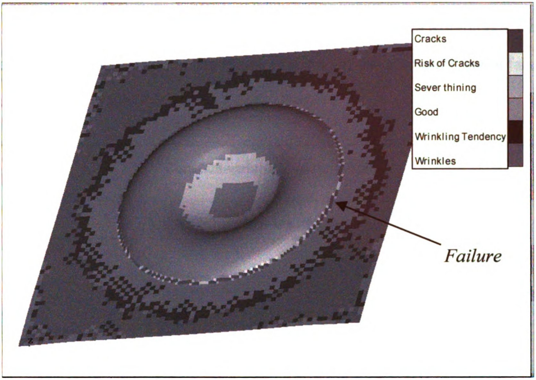

Figure 33. FLD results. Failure is predicted at the edges for a 3448 kPa (500 psi) pressure.

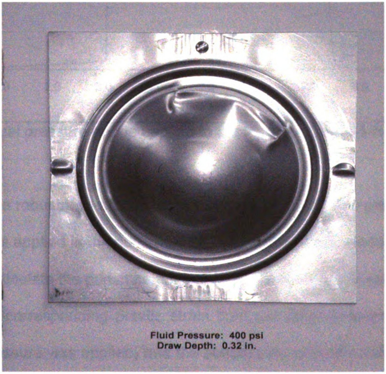

Figure 34. Pressure profile shown in Fig. 25 was applied to the topside of the sheet. Failure occurred at a draw depth of 0.32 in.

Figure 35 shows the actual fluid pressure curve used in the experiment, which was applied to the topside of the sheet, resulting in the premature sheet failure, as shown in Figure 34.

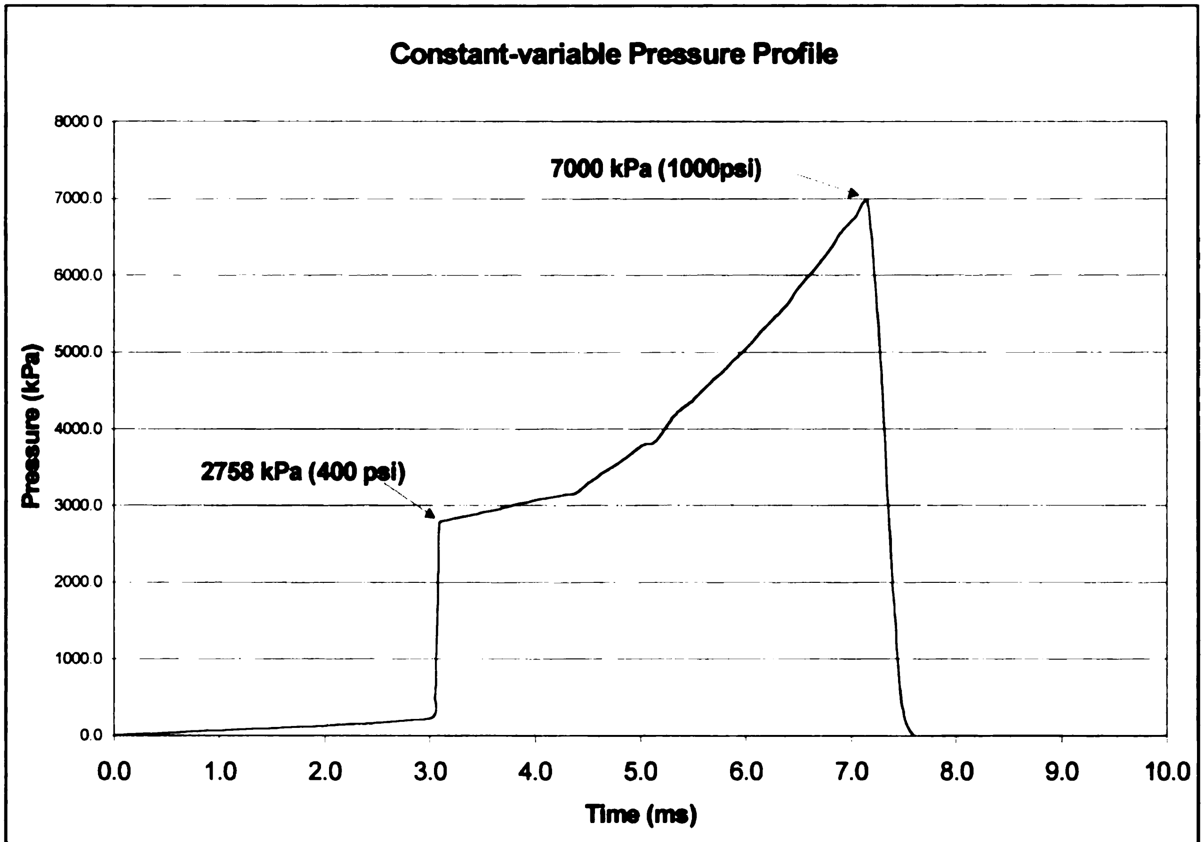

Figure 35. Actual pressure profile applied to the topside of a 3003-H14-aluminum sheet alloy.

To verify the robustness of the numerical modeling, the same pressure profile (Figure 35) was applied in the numerical analysis of the sheet, modeled with solid elements, to calculate the punch height and location where the sheet fails. Figure 36 shows the corresponding plastic strain contours developed on the topside (where the pressure was applied) and the bottom side of the hydroformed sheet. The model predicts that the aluminum sheet would fail at its corner radii on the topside (Figure 36(a)). This compares very well with the actual failure location observed in the experiment (Figure 34). The numerically predicted punch height at the failure point was 6.6mm (0.26in), which faired well against the experimental punch height of 8.1 mm (0.32").

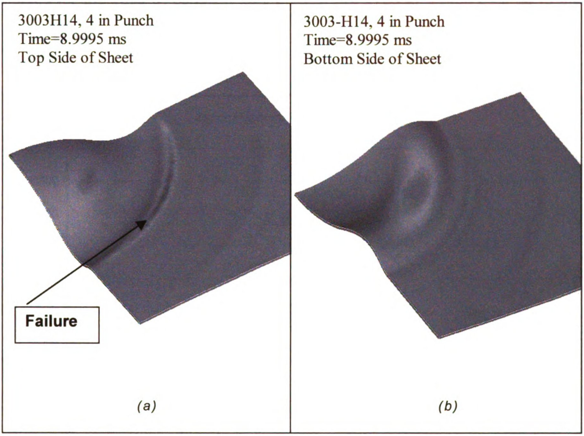

Figure 36. Plastic strain contours, predicted with a solid model, for a 3003-H14 aluminum sheet alloy after the pressure profile in Figure 34 was applied to its topside, (a) topside of the sheet, and (b) bottom side of the sheet.

In pure stretch experiments, with constant fluid pressure maintained throughout the whole process, a significant increase in the punch depth, before failure, was noticed (see Figure 14). The numerical model also predicts higher punch depths, before failure, when constant pressure is applied to the topside of the sheet.

Figure 37 shows the experimental and numerical punch force-displacement curves for the case of constant fluid pressure of 2758 kPa (400 psi), up to the failure point.

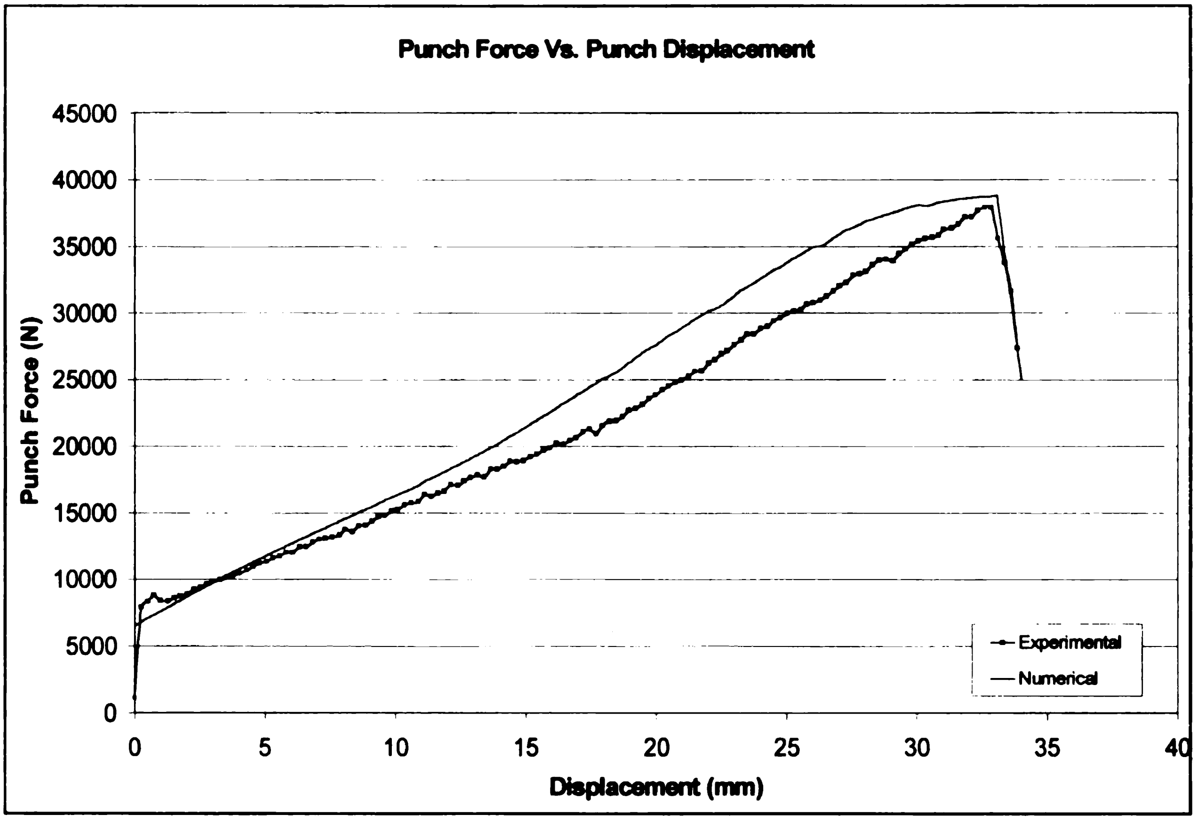

Figure 37. Punch force versus punch displacement for the 400 psi constant fluid pressure.

Figure 38 shows the numerical punch force-displacement plots, up to the failure point, for several constant fluid pressures for the AA3003-H14 material, while Figure 39 shows the similar plots for the AA6111-T4 material.

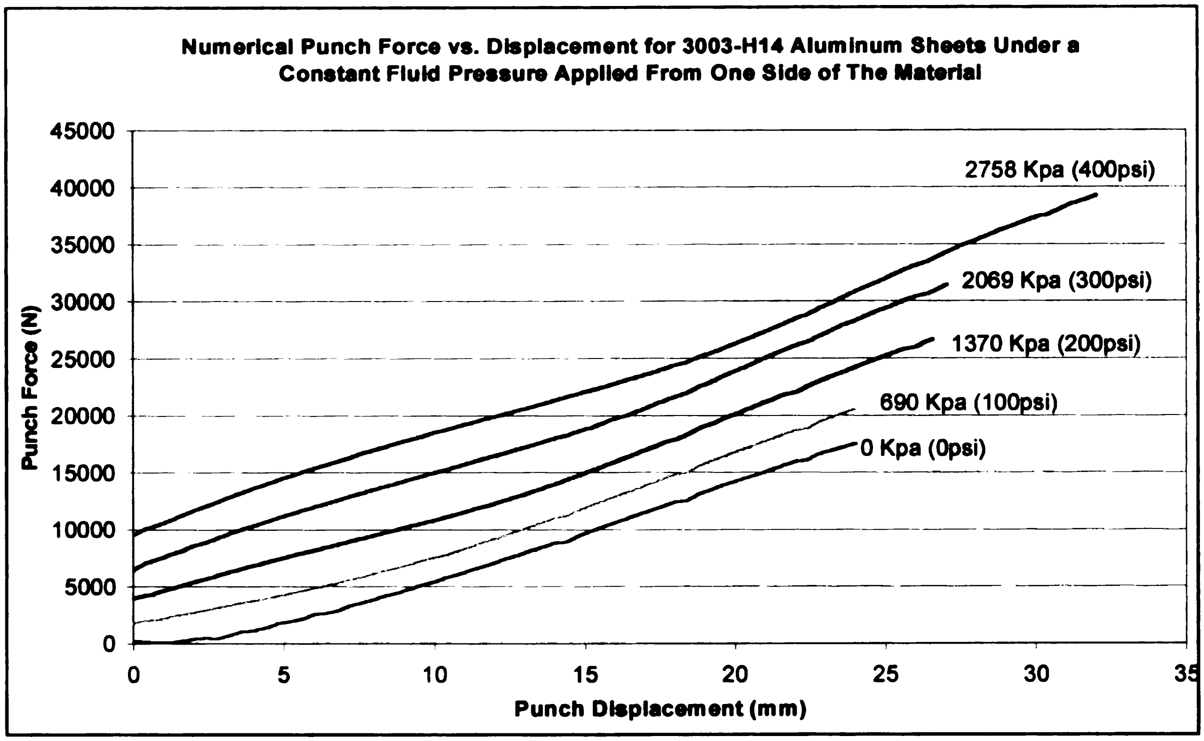

Figure 38. Numerical punch force-displacement results for aluminum 3003-H14-alloy sheet at constant fluid pressures applied to the topside of the sheet.

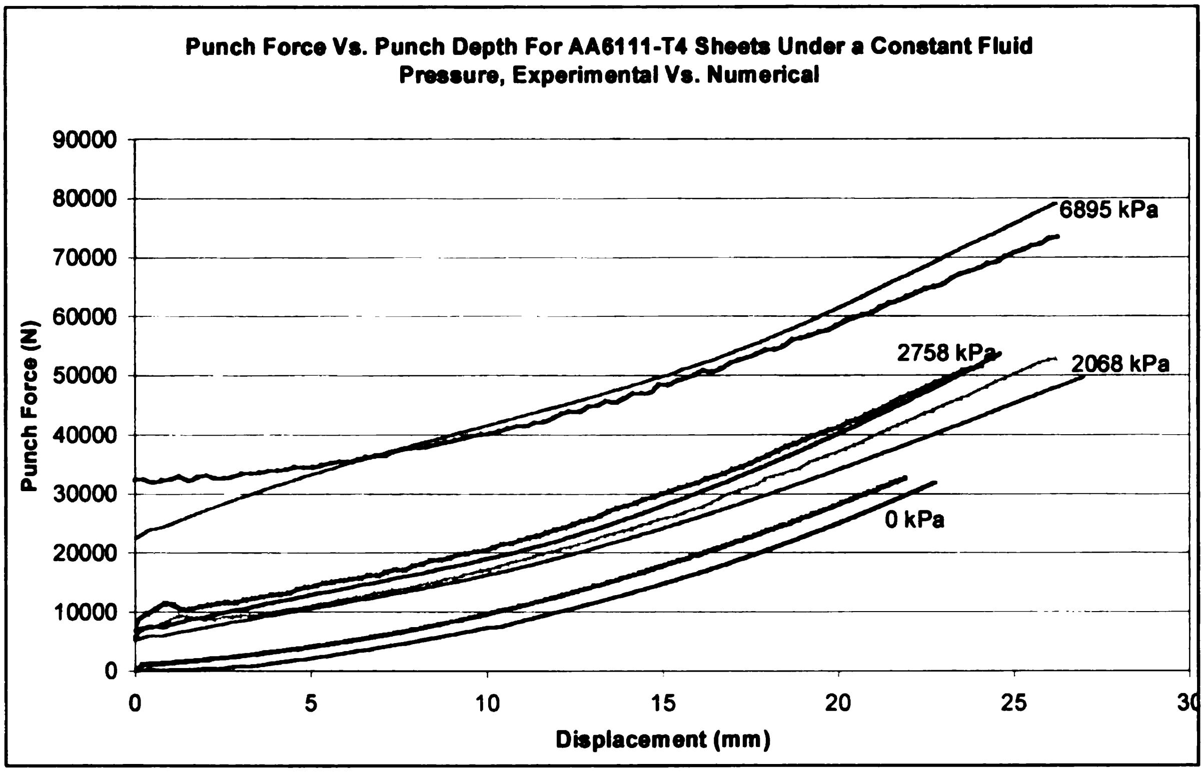

Figure 39. Numerical and experimental punch force-displacement results for AA6111-T4 sheets at constant fluid pressures applied to the topside of the sheet.

It is obvious that compared to conventional stamping (no fluid pressure), the hydroformed aluminum sheet reaches significantly deeper punch depths, before it fails. This increase in the punch depth improves with increasing the fluid pressure, up to a maximum value of 2758 kPa (400 psi). Besides the obvious improvement in the failure punch depth, the pressurized fluid also forces the sheet to conform to the shape of the punch more closely, resulting in a better formed part and a possible reduction in the springback, as shown in Figure 40.

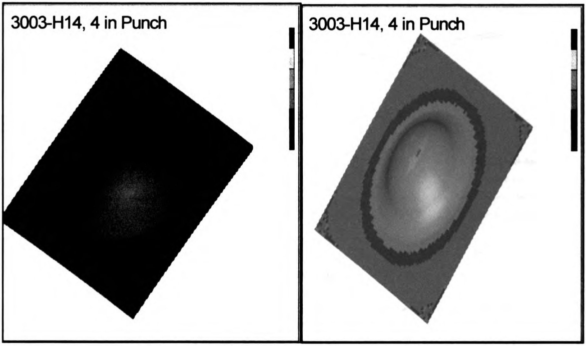

(a) 0 kPa Pressure
Failure Depth: 24mm

(b) 2758 kPa (400 psi)
Failure Depth: 32mm

Figure 40. Part shape comparison between: (a) conventional stamping (no fluid pressure), and (b) a hydroformed sheet with a constant fluid pressure of 2758 kPa (400 psi) applied to its topside.

Using the above method of determining the relationship between pressure and punch depth at failure (Figure 38 and 39), the upper limit of the optimum pressure-punch stroke path for the stamp hydroforming process (Figure 2) was determined. Figure 41 shows the experimental and numerical curve fit of the optimum pressure path determined for two punch sizes, 101.6 mm (4 in) and the 76.2 mm (3 in) punch.

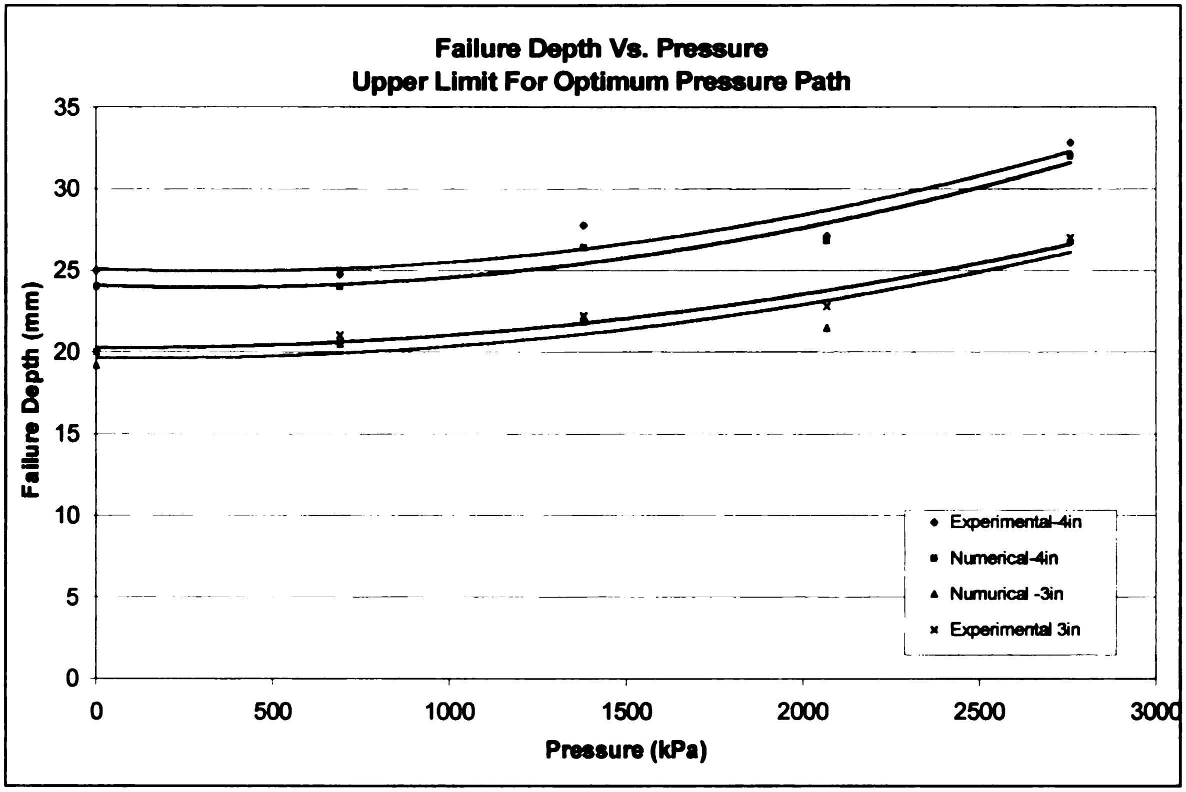

Figure 41. Experimentally and numerically determined upper limit of the optimum pressure-punch stroke path for the stamp hydroforming process.

6.1.3 Pure Stretch, Varying Fluid Pressure Applied to Topside of the Sheet:

In the case of varying fluid pressure, the pressure was applied to the topside of the sheet incrementally up to 14.4 MPa (2080 psi). In the numerical simulation, the punch was given a velocity profile, since in the experiments the punch was not stopped during the process of applying the fluid pressure. The fluid pressure profile applied in the numerical analysis was taken from the experimental data (see Figure 12(b)). The timing of the pressure profile was changed in order for it to be applied in the numerical analysis. Figure 42 shows the predicted punch force, before failure, matching the experimental values very well (3% error).

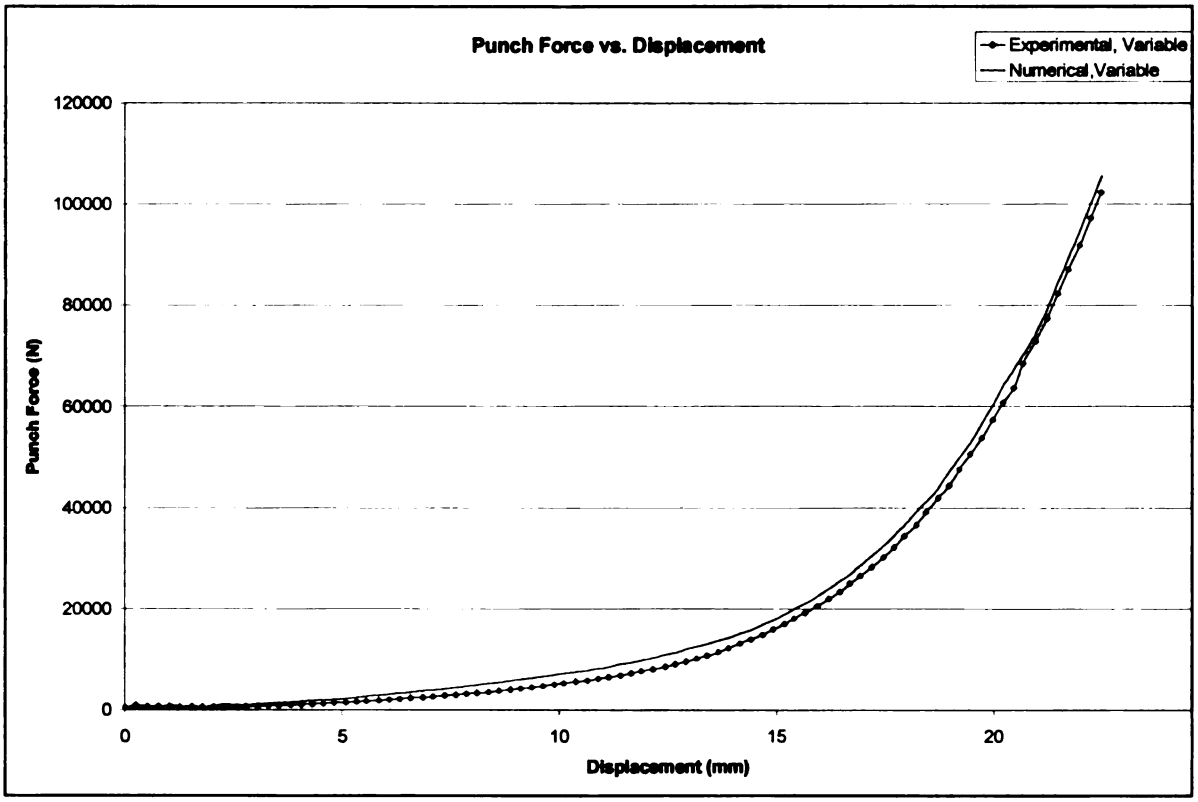

Figure 42. Punch force versus punch displacement for varying fluid pressure.

6.2 Deep Drawing

The idea behind these experiments evolved from the fact that an active blank holding force can prevent wrinkles from occurring in the blank holder region. The idea was to try to use the fluid pressure, used with a specific pressure profile, to work as the blank holding force. In this case no blank holder is required. The fluid pressure, applied using this method, has an advantage over an active blank holding force in that the whole blank is supported by the fluid pressure, and therefore wrinkles could be eliminated not just underneath the blank holder region, but also on the unsupported regions of the sheet. Also, better conformity to punch shape would be attained. Because of the limitations of the existing experimental setup, this idea was not yet tested experimentally, however, they were carried out only numerically. Based on the success of the results from the numerical model a new blank holder design that would enable the experimental verification of the numerical results was built.

First, wrinkling behavior of the sheet without fluid pressure will be investigated and the results of the numerical model will be compared to the experiments. After that, the effect of applying the fluid pressure will be investigated to find the suitable pressure profile. These tests were carried out using the 6111-T4 aluminum sheets.

6.2.1 Deep Drawing Without Fluid Pressure:

To induce wrinkling behavior in the sheet during forming, a constant distance of 4 mm (0.157 in) between the upper and lower blank holder was maintained. A low blank holding force was also used in other tests. As the punch traveled through the die cavity forming the sheet, inner instabilities and compressive forces in the sheet caused wrinkles to form. Wrinkles first appeared underneath the blank holder and then as the punch traveled further they increased and propagated into the cavity of the die. These initial experiments were used to validate the numerical model for the stamping of AA6111-T4 aluminum sheets under various conditions.

Figure 43 shows the experimental vs. numerical results for the AA6111-T4 when using a 2.0kN (450 lbf) BHF (blank-holder force) for forming the round sheet blank with the 76.2 mm (3 in) punch. It is clear that the numerical model captures the complex wrinkling behavior even when the sheet is formed to an extreme case. (In this case the punch depth is allowed to extend beyond what is normally required of the process). For the experiments using a constant displacement of 4mm between the die and blank holder the results for the 101.6 mm (4in) punch are shown in Figure 44. In Figure 45 the result for the 76.2 mm (3 in) Punch is shown. It is evident that the numerical model accurately predicted the location and even the exact number of wrinkles on the sheet during the stamping process.

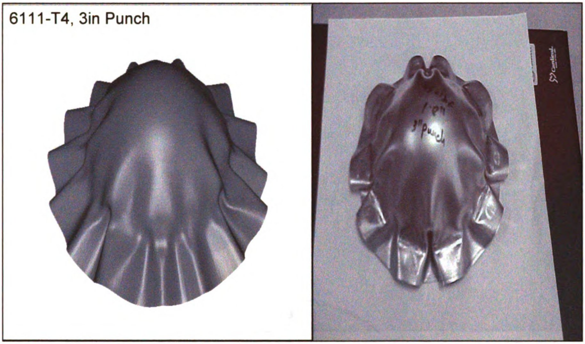

Figure 43. Wrinkling behavior of AA6111-T4 under 2.0 kN (450lbf) BHF. Numerical vs. experimental results.

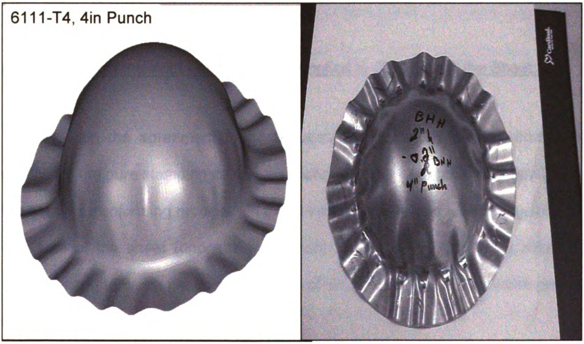

Figure 44. Forming with 101.6 mm (4in) punch. Number of wrinkles Numerical =20; Experimental =20.

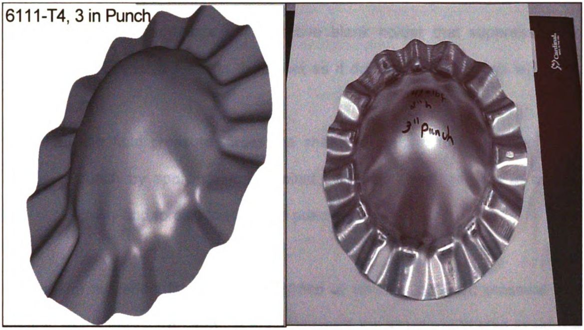

Figure 45. Forming with 76.2 mm (3in) punch at 450lbf BHF. Number of wrinkles Numerical =15; Experimental =15.

6.2.2 Deep Drawing With Fluid Pressure Applied to One Side of the Sheet:

Based on the agreement found between the numerical and experimental results for the pure stamping cases, the model created was confidently applied to the stamp hydroforming process. In these simulations, a pressure was applied to one side of the sheet (opposite the punch) to simulate a pressure controlled blank holding force on the sheet. The use of an appropriate fluid pressure profile benefits in two ways:

1. The pressure acts as an active blank holder that suppresses the compressive force in the sheet as it deforms which delays wrinkling, and
2. The fluid pressure forces the sheet to conform to the shape of the punch by applying work against the unsupported regions in the die cavity and forcing them to the punch profile.

Several numerical tests were performed at which a constant pressure was applied to the sheet. The forming depth at which the sheet would start to wrinkle was recorded. The wrinkles were observed visually.

Since the pressure in this case will depend on the initial geometry, especially the area underneath the blank holder, tests were made using the two punch sizes (3 and 4 in) and with multiple initial round blank diameters. The ratio of the initial blank diameter (b_0) to the diameter of the punch (a) was used as a method to generalize the pressure profile to other experiments. Using this method a pressure profile was extracted for different initial blank size to punch diameter ratios. Figure 46 shows the results for three different ratios. It should be noticed that the pressure profile depends on the initial size of the blank and the punch diameter. This is in agreement with the theoretical lower pressure profiles limits suggested by Yossifon and Tirosh (1977–1988) [8–12].

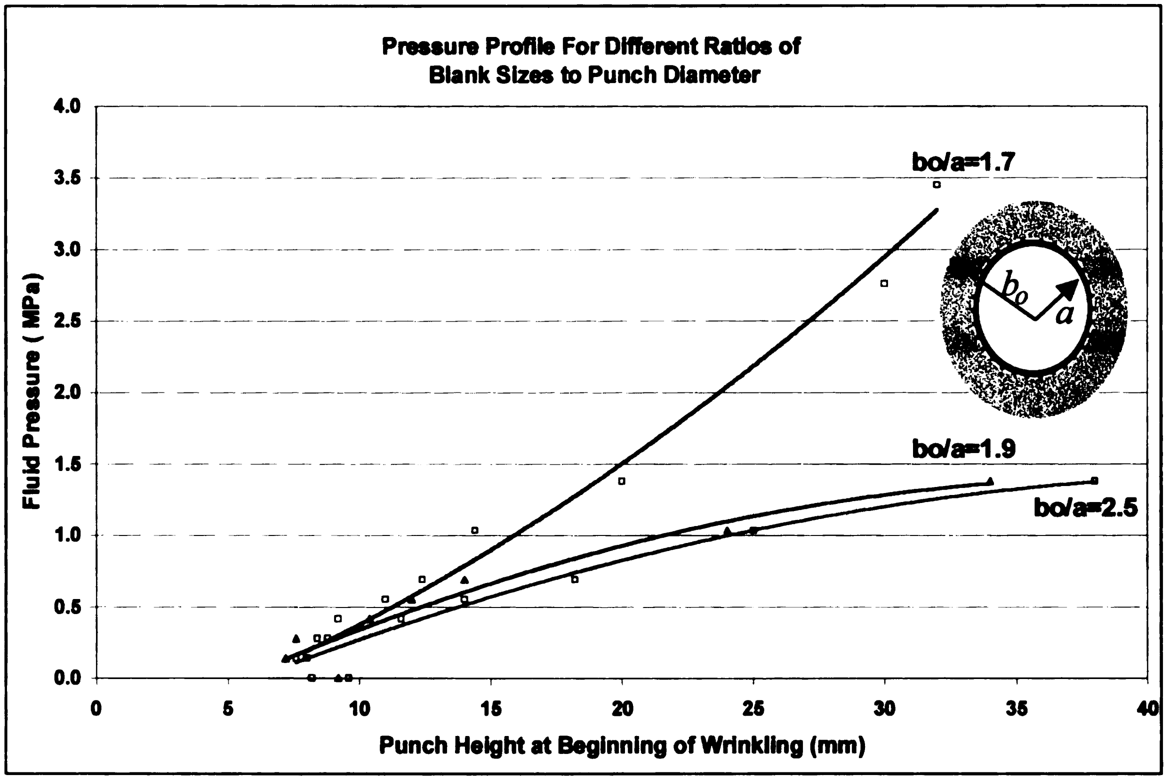

Figure 46. Pressure profile extracted for wrinkling ironing for different initial blank size to punch diameter ratios.

After acquiring the pressure profiles, their accuracy had to be tested. A method to do that was to take the same pressure profile and use it in the numerical model instead of a constant pressure profile to test whether it will prevent the sheet from wrinkling. However, after applying the pressure using this method, it was noticed that the wrinkles were not ironed out and they still occurred.

Considering that wrinkling is an instability that occurs when compressive stresses in the plane of the sheet reach a specified limit, it is absolutely necessary to prevent wrinkling from ever initiating in the first place. By re-examining the curve fitting method used in Figure 46, it becomes obvious that some of the predicted wrinkling points are above the curve fit. Naturally, by using those curve fits as the optimum pressure profile, it is not possible to prevent wrinkles from forming.

Using this knowledge, the same pressure profiles were adjusted so that the pressure is applied earlier with respect to punch depth. Figure 47 shows this method for the b_O/a=1.7 setup.

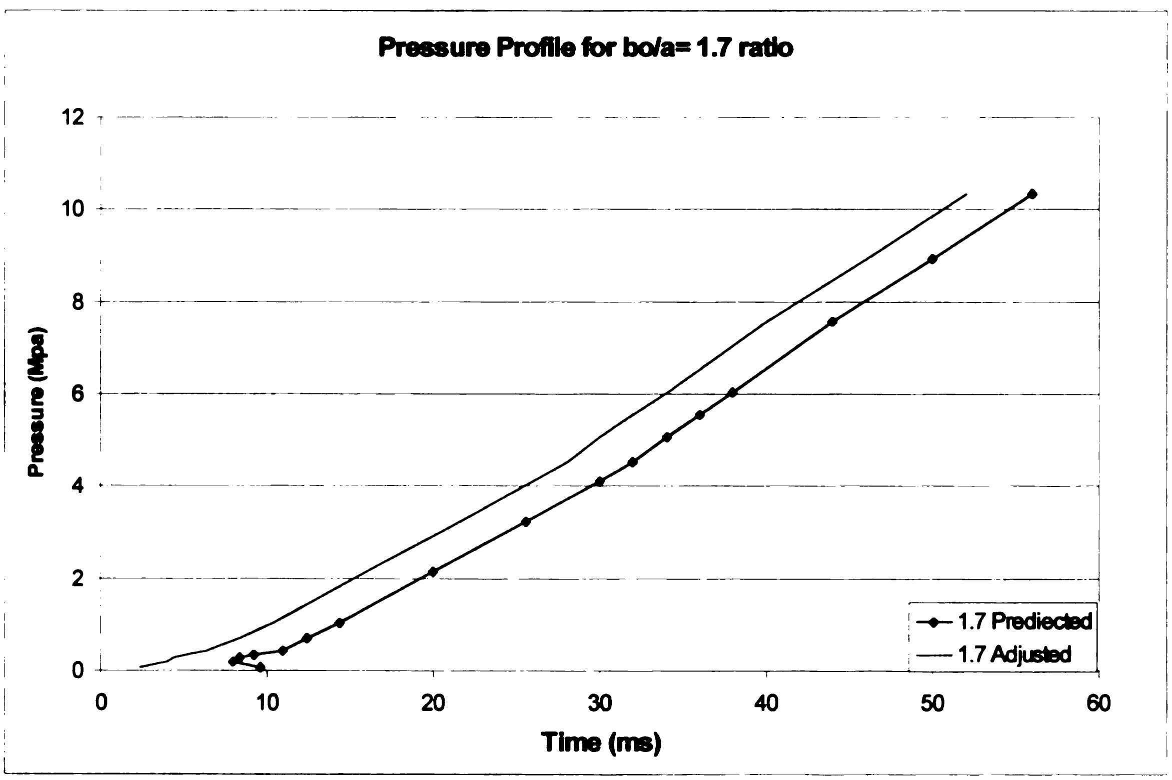

Figure 47. Adjusted pressure profile.

Figure 48 shows the effect of applying fluid pressure to one side of the sheet with a displacement controlled blank holder set at 4mm (0.157 in) from the lower die for the 101.6 mm (4 in) punch using the adjusted pressure profile shown in Figure 47. It is clear that the wrinkles have been ironed out; also, a better forming behavior in the form of better overall shape and final sheet thickness distribution is achieved using this method.

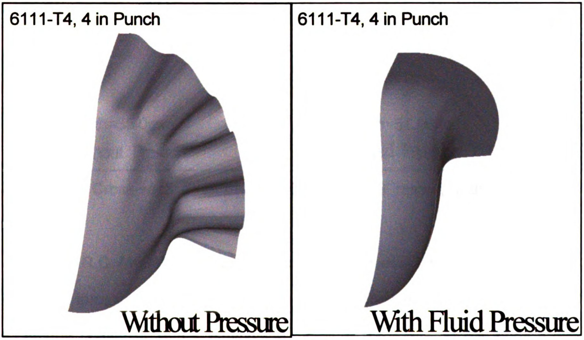

Figure 48. Effect of using Fluid pressure on wrinkling. (101.6 mm Punch).

A cross section of the previous shape is shown in Figure 49. Without fluid pressure, not only there is a poor conformity to the punch shape, but also the sheet ruptures earlier in the process when compared to the hydroforming case. Draw depths achieved without rupture, but with wrinkling occurring, were 35 mm

(~1.4 in) with no fluid pressure versus 51 mm (~2 in) for the stamp hydroforming case and without wrinkling either underneath the blank holder or in the unsupported region between the punch and the die.

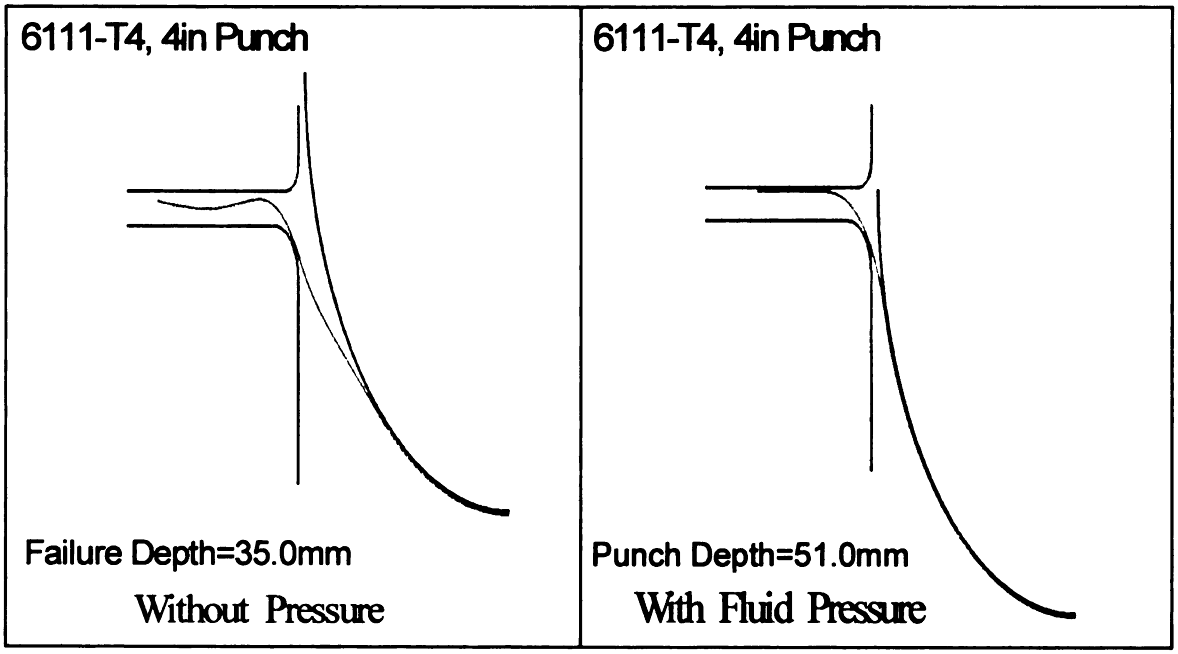

Figure 49. Cross-section of the 101.6 mm (4 in) punch, without and with pressure.

Becker R.C. (1996) [39] made a study on factors affecting surface roughness in sheet forming where he used the micromechanics finite element model technique combined with a polycrystal model of the sheet. In the study it was found that strains in the sheet during the forming process are much higher when the sheet is in a biaxial tension case than when it is in a uniaxial tension case, shown in Figure 50. Therefore, the sheet metal will rupture much faster when it is in a biaxial tension condition due to higher strains in the sheet than if it is in a uniaxial tension condition.

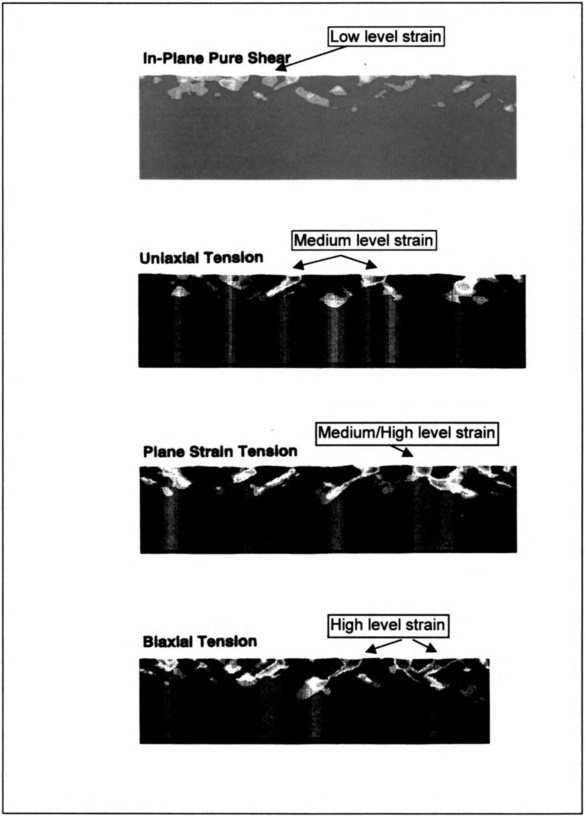

Figure 50. Contours of maximum principle logarithmic strains for several strain paths [39].

The Forming Limit Diagram (FLD) displaying contour plots of the minor and major strains developing in the hydroforming process with the 101.6mm (4 in) punch is shown in Figure 51. From this figure it is shown that applying the fluid pressure causes a drastic change in the strain distribution of the formed part as compared with the case of sheet forming without the assistance of the fluid pressure. Also it should be noticed that in the case with fluid pressure the strains are well below the failure limit, while in the case without the fluid pressure the material fails (squares crossing the upper limit line) early on.

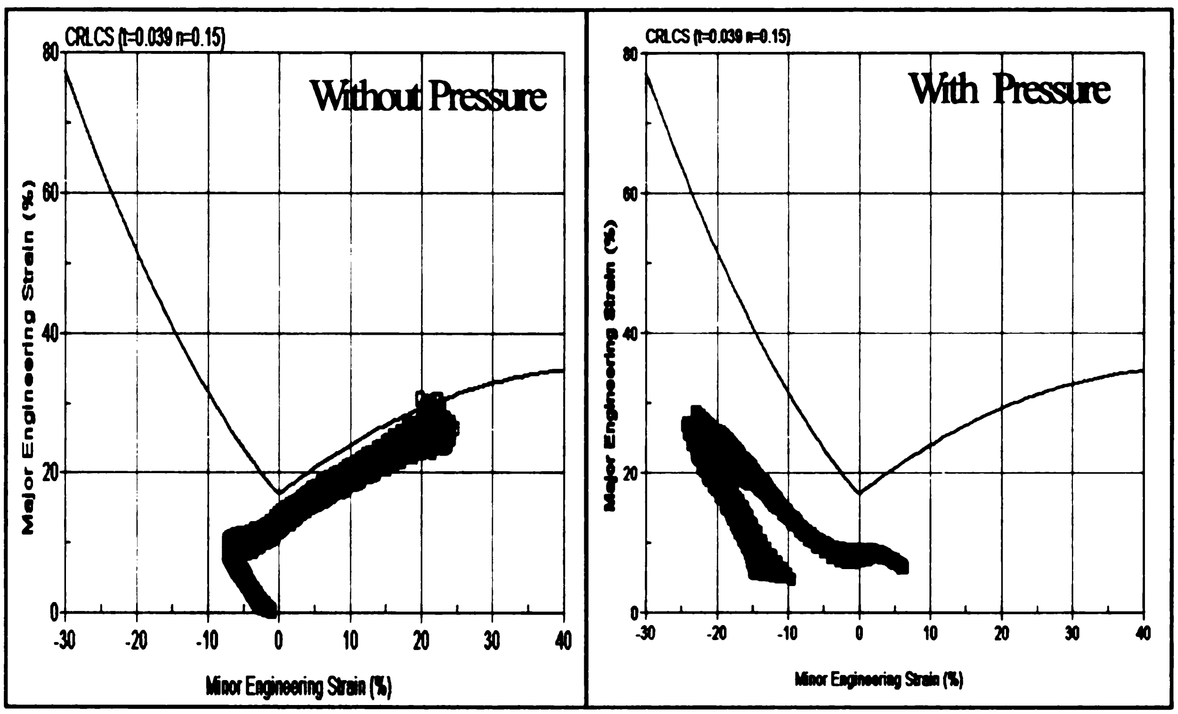

Figure 51. FLD Failure and distribution of strains for the 101.6 mm (4in) punch case.

In the case without the fluid pressure, it is noticed that the strains in the sheet are in the biaxial tension region, while applying the fluid pressure to the sheet during the forming process moved the strains in the sheet to the uniaxial (left) region. This redistribution of strains caused a deeper drawing of the sheet without rupturing it, as compared to the case of forming without fluid pressure where the sheet was in the biaxial tension condition. These results are in good agreement with Becker's micromechanics modeling results [39], as shown in Figure 50.

6.2 New Blank Holder Design

The results obtained from the numerical analysis of the deep drawing with fluid pressure applied to one side of the sheet (Section 6.2.2) needs to be verified experimentally. The current experimental setup does not allow the process of drawing the sheet and at the same time keeping the pressurized fluid contained.

From the numerical modeling, a new sheet drawing setup was designed that would allow a displacement control of the blank holder while maintaining the pressure inside the fluid chamber. This new design is shown in Figure 52. This design will allow the material to draw in, and at the same time contains the fluid in the lower chamber by means of a seal. This part was built very recently (April 2002) and installed on the stamping press, as shown in Figure 53. No experiments have yet been performed to verify the numerical results shown in Figure 48.

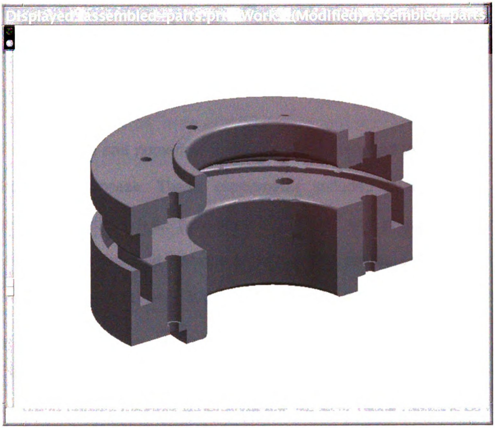

Figure 52. New blank holder design.

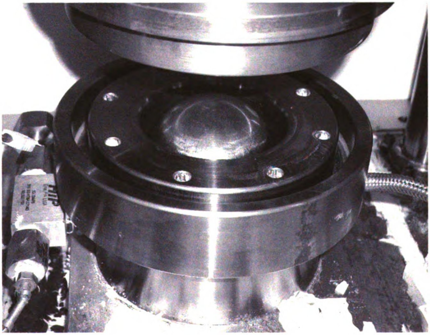

Figure 53. Actual new blank holder design installed.

Chapter 7

CONCLUSIONS

Experimental and numerical analyses were conducted to evaluate the sheet hydroforming process. These experiments included studying the effect of boundary conditions (i.e., pure-stretch, draw-in) and pressure loadings (i.e., constant and varying fluid pressure and a localized pressure applied using a vinyl sheet) on the deformation of 3003-H14 and 6111-T4-aluminum sheet alloys.

Numerical analyses of the hydroforming process conducted with LS-Dyna 3D code, using correct material proprieties and material model, were able to capture the failure and wrinkling characteristics of the aluminum sheet alloys very well. The accuracy of the numerical predictions were very sensitive to the material properties of the sheet metal. To correctly capture the wrinkling behavior of the sheet, it was necessary to use an anisotropic material model.

By comparing experimental results without fluid pressure to numerical ones, an accurate numerical modeling capability to predict wrinkle formation in sheet metals was established. Using this same model and expanding it to simulate fluid pressure tests it was found that stamp hydroforming could be used as a viable alternative forming process not only capable of preventing wrinkles, but also of increasing the formability and drawing depths for the final required shape. It should be emphasized that the success of the process requires a specially derived fluid pressure profile to prevent both wrinkling and rupturing instabilities from occurring.

The lower and upper limits of the optimum fluid pressure-punch stroke path for the stamp hydroforming of aluminum sheet metals was determined, see Figure 2. The upper limit was proven both excrementally and numerically. The lower limit of the pressure profile was only proven numerically due to the limited capabilities of the current experimental setup. A new blank holder is designed based on the numerical analysis and installed on the experimental setup for verification of the pressure profile. The experiments verifying the lower pressure profile will be conducted in the future.

REFERENCES

References

[1] Cao J. and Boyce M.C., "A Predictive Tool for Delaying Wrinkling and Tearing Failures in Sheet Metal Forming", Journal of Engineering Material and Technology, Vol. 119, pp. 354-365, 1997.

[2] Kawaka M., Olejnik L., Rosochowski A., Sunaga H. and Makinouchi A. "Simulation of Wrinkling in Sheet Metal Forming", Journal of Materials Processing Technology, Vol. 109, pp. 283-289, 2001.

[3] McClintock, F.A. "A Criterion for Ductile Fracture by the Growth of Holes", Journal of Applied Mechanics, Vol. 35, pp. 363-371, 1968.

[4] Rice, J.R. and Tracey, D.M. "On the Ductile Enlargement of Voids on Triaxial Stress Fields", Journal of Mechanical Physics and Solids, Vol. 17, pp. 201-217, 1969.

[5] Clift, S.E., Hartley, P., Sturgess, C.E.N. and Rowe, G.W. "Fracture Prediction in Plastic Deformation Process", International Journal of Mechanical Sciences, Vol. 32, No. 1, pp. 1-17, 1990.

[6] Hartley, P., Pillinger, I. and Sturgess, C. "Numerical Modeling of Material Deformation Processes Research Development and Applications", Springer-Verlag, 1992.

[7] Youssef, Y. and Denault, J. "Thermoformed Glass Fiber Reinforced Polypropylene: Microstructure, Mechanical Properties and Residual Stresses", Polymer Composites, Vol. 19, No. 3, pp. 301-309, 1998.

[8] Tirosh, J., Yossifon, S., Eshel, R. and Betzer, A. "Hydroforming Process of Uniform Wall Thickness Products", ASME Journal of Engineering for Industry, Vol. 99, pp. 685-691, 1977.

[9] Yossifon, S., Tirosh, J. and Kochavi, E. "On Suppression of Plastic Buckling in Hydroforming Processes", International Journal of Mechanical Sciences, Vol. 26, pp. 389-402, 1984.

[10] Yossifon, S. and Tirosh, J. "Rupture Instability in Hydroforming Deep-Drawing Process", International Journal of Mechanical Sciences, Vol. 27, pp. 559-570, 1985.

[11] Yossifon, S. and Tirosh, J. "Buckling Prevention by Lateral Fluid Pressure in Deep Drawing", International Journal of Mechanical Sciences, Vol. 27, pp. 177-185, 1985.

[12] Yossifon, S. and Tirosh, J. "On the Permissible Fluid-Pressure Path in Hydroforming Deep Drawing Processes - Analysis of Failures and Experiments", Journal of Engineering for Industry, Vol. 110, pp. 146-152, 1988.

[13] Lo, S.W., Hsu, T.C. and Wilson, W.R.D. "An Analysis of the Hemispherical-Punch Hydroforming Process", Journal of Materials Processing Technology, Vol. 37, pp. 225-239, 1993.

[14] Hsu, T.C. and Hsieh, S.J. "Theoretical and Experimental Analysis of Failure for the Hemisphere Punch Hydroforming Processes", Journal of Manufacturing Science and Engineering, Vol. 118, pp. 434-438, 1996.

[15] Gelin, J.C., Delassus, P. and Fontaine, J.F. "Experimental and Numerical Modeling of the Effects of Process Parameters in the Aquadraw Deep Drawing", Journal of Materials Processing Technology, Vol. 45, pp. 329-334, 1994.

[16] Gelin, J.C., Ghouati, O. and Paquier, P. "Modeling and Control of Hydroforming Processes for Flanges Forming", CIRP Annals - Manufacturing Technology , Hallwag Publ Ltd, Berne, Switzerland, Vol. 47, No. 1, p 213-216, 1998.

[17] Baida, M., Gelin, J.C. and Ghouati, O., 1999, "Modeling the Hydroforming of Thin Metallic Components", Proceedings of the Seventh International Symposium on Plasticity and Its Current Applications (PLASTICITY '99), Edited by Khan A., Cancun, Mexico, January 5-13, pp. 293-296.

[18] Shang, H.M., Qin, S. and Tay, C.J. "Hydroforming Sheet Metal with Intermittent Changes in the Draw-In Condition of the Flange", Journal of Materials Processing Technology, Vol. 63, pp. 72-76, 1997.

[19] McClintock, F.A. "A Criterion for Ductile Fracture by the Growth of Holes", Journal of Applied Mechanics, Vol. 35, pp. 363-371, 1968.

[20] Geckler J.W. "Plastisches Knicken der Wandung von Hohlzylnder und einige Faltungsverscheinungen an Schalen und Blechen", Ziet. Andew. Math. Mech., Vol. 8, pp. 341-352, 1924.

[21] Baldwin W.M Jr. and Howald T.S. "Folding in the Cupping Operation ", Transactions of A.S.M., Vol. 38, pp. 757-788, 1947.

[22] Senior B.W. "Flange wrinkling in Deep-Drawing Operations", Journal of Mechanical Physical Solids, Vol. 4, pp. 235-246, 1981.

[23] Yoshida K, Hayashi H., Hirata M., Hira T. and Ujihara S. "Yoshida Buckling Test", IDDRG Paper, DDR/WG III/81, Japan, 1981.

[24] Triantafyllidis N. and Needlmen A. " An Analysis of Wrinkling in the Swift Cup Test", Journal of Engineering Materials Technology, Vol. 102, pp. 241-248, 1980.

[25] Doege E., El-Dsoki T. and Seibert D. "Prediction of Necking and Wrinkling in Sheet-Metal Forming", Journal of Material Processing Technology, Vol. 50, pp. 197-206, 1995.

[26] Wang X. and Cao J. " On the Predication of Side-Wall Wrinkling in Sheet Metal Forming Processes", International Journal of Mechanical Sciences, Vol. 42, pp. 2369-2394, 2000.

[27] Chung K. and Shah K. " Finite Element Simulation of Sheet Metal Forming for Planer Anisotropic Metals", International Journal of Plasticity, Vol. 8, pp. 453-476, 1992.

[28] Barlat F., Lege D.J. and Brem C. " A Six-Component Yield Function for Anisotropic Materials", International Journal of Plasticity, Vol. 7, pp. 693-712, 1991.

[29] Kim J.B., Yang D.Y., Yoon J.W. and Barlat F. " The Effect of Plastic Anisotropy on Compressive Instability in Sheet Metal Forming", International Journal of Plasticity, Vol. 16, pp. 649-676, 2000.

[30] Kim J.B., Yoon J.W., Yang D.Y. and Barlat F. " Investigation into Wrinkling Behavior in the Elliptical Cup Deep Drawing Process by Finite Element Analysis Using Bifurcation Theory", Journal of Materials Processing Technology, Vol. 111, pp. 170-174, 2001.

[31] Kawka M., Olejnik L., Rosochowski A., Sunaga H. and Makinouchi A. "Simulation of wrinkling in Sheet Metal Forming", Journal of Materials Processing Technology, Vol. 109, pp. 283-289, 2001.

[32] Zampaloni M. "Experimental and Numerical Study of Stamp Hydroforming for Processing Glass Mat Fiber Reinforced Thermoplastic Sheets", Master of Science Thesis, Michigan State University, 2000.

[33] United States Patent Pending.

[34] LSTC Web Site. www.lstc.com

[35] Zampaloni M., Abedrabbo N. and Pourboghrat F. "Experimental and Numerical Study Of Stamp Hydroforming Of Sheet Metals" Submitted to International Journal of Mechanical Sciences, 2002

[36] Abedrabbo N., Zampaloni M. and Pourboghrat F. "Numerical Study Of Wrinkling Behavior Of Al6111-T4 In Stamp Hydroforming" submitted to The fifth international conference and workshop on numerical simulation of 3D sheet forming processes NUMISHEET2002, Korea, 2002.

[37] Hosford, W.F. and Caddell, R.M. "Metal Forming – Mechanics and Metallurgy", Prentice-Hall, Inc., 1983

[38] Barlat F., Mayed Y., Chung K., Yanagawa M., Brem C.J., Hayashida Y., Lege D, Matsui K, Murtha S., Hattori S., Becker R. and Makosey S. "Yield Function Development For Aluminum Sheet Alloys", Journal of Mechanical Physical Solids, Vol. 45m No 11/12, pp. 1727-1763, 1997.

[39] Becker R.C., "Factors Affecting Surface Roughening in Sheet Forming", ALCOA Technical Center Report No. 96-12-002, 1996.